DEVELOPMENT AND CHARACTERIZATION OF CoFeNi-WC COMPOSITE

By

M Muneeb ur Rehman

M Ali Siddique

Huzaifa Mehmood

School of Chemical and Materials Engineering

National University of Sciences and Technology

2022

DEVELOPMENT AND CHARACTERIZATION OF CoFeNi-WC COMPOSITE

By

(Leader – 264865 M Muneeb ur Rehman)

(Member 1 – 254683 M Ali Siddique)

(Member 2 – 260667 Huzaifa Mehmood)

A THESIS

Submitted to

National University of Sciences and Technology

In partial fulfilments of the requirements

for the degree of

METALLURGICAL AND MATERIAL ENGINEERING

School of Chemical and Materials Engineering

National University of Sciences and Technology

June , 2022

CERTIFICATE

This is to certify that work in this thesis has been completed by Mr. M Muneeb ur Rehman, Mr. M Ali Siddique and Mr. Huzaifa Mehmood under the supervision of Dr Khurram Yaqoob at the school of Chemical and Materials Engineering (SCME), National University of Science and Technology, H-12, Islamabad, Pakistan.

---------- ----------

Advisor: Co-Advisor (if any)

Dr. Khurram Yaqoob
Department of Materials Engineering
School of Chemical and Materials Engineering
National University of Sciences and Technology

Submitted Through:

HOD----------

Department of Materials Engineering
School of Chemical and Materials Engineering
National University of Sciences and Technology

Principal/Dean ----------
School of Chemical and Materials Engineering
National University of Sciences and Technology

DEDICATION

Dedicated to our beloved parents and family who are reason for our success and happiness

ACKNOWLEDGMENT

All glory and appreciations for ALLAH ALMIGHTY for HIS countless blessings that made us complete this research project and thesis on time.

We are thankful to our beloved parents for their prayers, support, and encouragement. We are also grateful to our respected Supervisor Dr Khurram Yaqoob for his unparalleled support, dedication and mentoring which enabled us to complete this project and made us acquire skills necessary for a researcher and metallurgist. Moreover, we are also thankful to Mr. Shoaib and Mr. Adil who supported us in this project. Last but not the least we are grateful to NUST for giving us the opportunity for enhancement of skills and financial support.

ABSTRACT

An optimum combination of strength and toughness is required in many applications. A composite material can be synthesized with tailored properties by varying the amount of reinforcement in a matrix. CoFeNi was selected as the matrix to provide ductility and toughness to the composite. Composition of the ternary alloy was equi-molar which lies in the FCC range in the phase diagram. FCC was preferred as it is more ductile than BCC, HCP and intermetallic phases due to its active slip systems. WC particulates were added as a reinforcement to impart strength to the composite. The amount of WC added to the matrix was 1.0 and 2.0 wt.% and its effect on strength was studied. Characterization revealed an increase in hardness of the composite with addition of WC in the matrix

TABLE OF CONTENTS

LIST OF FIGURES

LIST OF TABLES

CHAPTER 1

INTRODUCTION

1.1 Composite Materials

Materials are basically divided into three categories: Metals, Ceramics, and Polymers. Composite materials are made up of two phases with strong interfacial connection between two of above. They are made up of a continuous phase called "Matrix" and a discontinuous phase called "Reinforcement" that consists of particles, fibres, and whiskers. Composites have showed higher mechanical characteristics as compared to monolithic alloys. They have better wear resistance, corrosion resistance, hardness, strength-to-weight ratio, stiffness, temperature stability, and thermal and electrical conductivity. There are two levels of classification for composites [1]. The first classification is based on the reinforcement morphology, as shown in Figure 1-1 below:

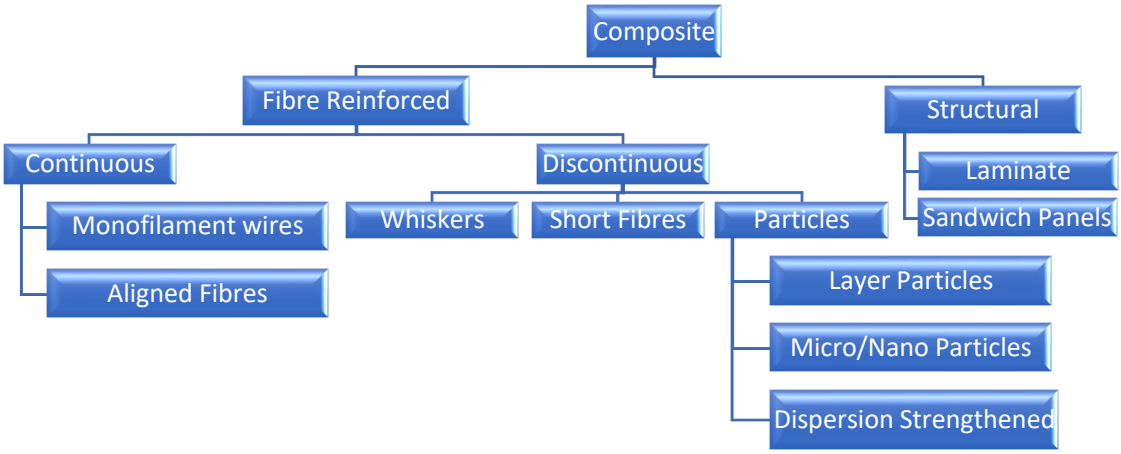

Figure 1. 1: Classification of composite based on type of reinforcement

The second distinction is frequently addressed in terms of the matrix's material composition. Metal Matrix Composites (MMCs), Ceramic Matrix Composites (CMCs), and Organic Matrix Composites (OMCs) are the three basic classes

covered by this description (OMCs). Both Polymer Matrix Composites (PMCs) and Carbon Matrix Composites are included in the term Organic Matrix Composites. The purpose of this study is to focus on MMC, which will be explained in the next chapter.

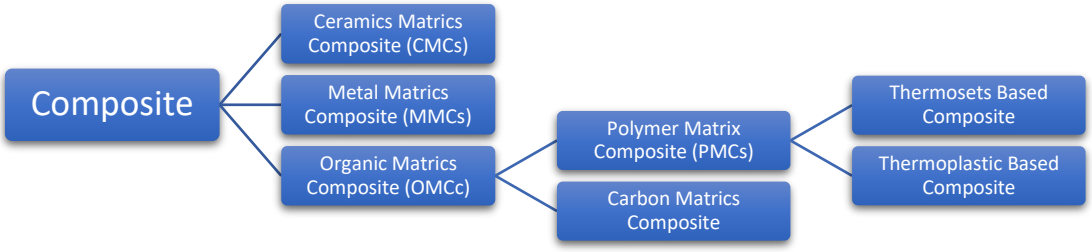

Figure 1. 2 : Classification of composite based on different matrix

1.1.1 Reasons of attraction for Composite Materials

Engineers and designers may benefit from composites in a variety of ways, including [2]:

- An-isotropic materials have the freedom to have specific qualities exclusively in preferred directions, i.e. an-isotropic materials.
- Quasi-isotropic materials have the same properties in-plane regardless of direction.
- Materials created to order for a specific purpose.
- Composite materials are more resistant to corrosion than metals.
- Composite's fatigue resistance is its strength.
- Less expensive to assemble than traditional materials.
- Weight reduction in goods that can be up to 50% less than metals, with the potential to go even lower.

A composite material is made up of a fibre or filament material and a matrix material in construction. The use of these materials has a specific function, and the goal of their application differs from one to the next. Reinforcement materials are primarily used to carry most of the load that is applied to the material. They also provide improved structural qualities like as thermal stability, stiffness, and strength. They are also responsible for electrical conduction within a composite. The matrix material's job is to hold the fibres together. The matrix material in a composite provides surface quality as well as structural stability. When it comes

to the creation of composites, shear characteristics are crucial since they inhibit fracture propagation and fibre degradation.

1.1.2 Metal Matrix Composites (MMC)

Metal matrix composites (MMCs) are made up of a metal matrix and some reinforcement. In order to build a material with increased qualities in contrast to unreinforced metals, they combine the best attributes of two distinct materials, such as toughness and ductility received from metal matrix and strength and modulus generated from ceramic reinforcements. MMCs are further classified into two types:

- Particulate Composite
- Fibre Reinforced

Our main focus will be on particle reinforcement, in which the embedded materials are equiaxed particulates with almost isotropic characteristics. When a metal matrix is strengthened with ceramic material, "cermet" is created. The following is a rule for mixing reinforcement into the matrix:

$$mc = mf + mm$$

Where **m** stands for mass, **c** for composite, **f** for filler, and m for matrix [3]. Because of the isotropic and spontaneous particle dispersion, strengthening ceramics in metal alloys improves the mechanical characteristics of the metal matrix.

MMCs (metal matrix composites) have been identified as one of the most important materials. They have better qualities than unreinforced materials and may be used to create materials with a higher strength-to-weight ratio, higher fatigue resistance, hardness, lower coefficient of friction, and lower thermal expansion coefficient. Aerospace, automotive, undersea equipment, and structural applications have all utilised MMCs. Metal matrix supplemented with nanomaterials has made the field of composite materials significantly more enticing for scientists in the previous decade. They've found their way into a variety of applications in the maritime, aviation, electronics, and automotive sectors.

The interaction of MMCs with nanomaterials like graphene, fullerene, and carbon nanotubes has piqued the interest of scientists all over the world, and attempts are being made to create metal nano composites with excellent mechanical, electrical, and thermal characteristics [4]. However, the reinforcing of nano carbon is highly dependent on process parameters and good process management to get optimal outcomes. Figure 1-3 depicts the various MMC manufacturing techniques available, with liquid metal infiltration by vacuum melting being used for this study.

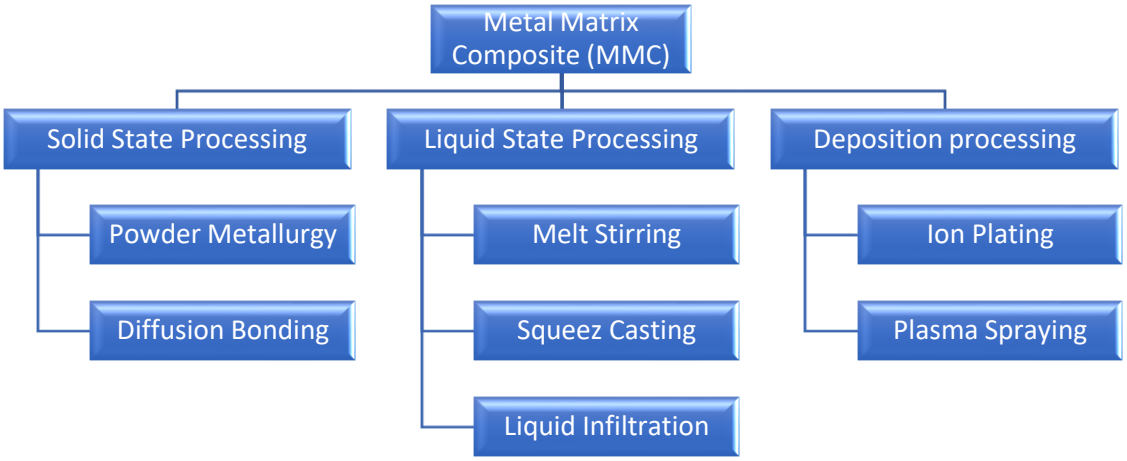

Figure 1. 3 : Fabrication routes for metal matrix Composites

In applications requiring exposure to high temperatures and other harsh environmental conditions, they outperform polymer matrices [5]. Metal Matrix Composites (MMCs) have seen a significant growth in research and development in the last decade or so due to:

- Enhanced fatigue, wear, and heat resistance, as well as improved strength and modulus
- In compared to unreinforced alloys, increased consistency in performance and characteristics.

The downside of MMCs is that they might cause undesirable chemical reactions at the fibre-matrix interface, creating intermetallic compounds that can interfere with load transmission to reinforcements and function as crack nucleation sites.

Given the tremendous potential for improving the thrust-to-weight ratio of aerospace, space, and automotive engines, a lot of attention has been paid to the development of lighter MMCs made of high entropy alloys[6].

1.2 Ternary Alloy as Matrix

1.2.1 Alloy

An alloy can be defined as the blend of different metals and other chemicals elements. Which may be a single phase (solid solution) of metal elements or a mixture of two or more solutions with well defined crystal structure.

1.2.2 Ternary Alloys

A ternary alloy is a combination of three elements, where the resulting material has different metallic properties from those of its components. An alloy is a combination of a metal with at least one other metal or non-metal. A system with 3 metallic components is referred to as a ternary alloy[7]. Due to 3 components, configurational entropy of ternary alloy is higher than binary alloys, hence it's stability is also higher. This higher stability corresponds to enhanced mechanical properties.

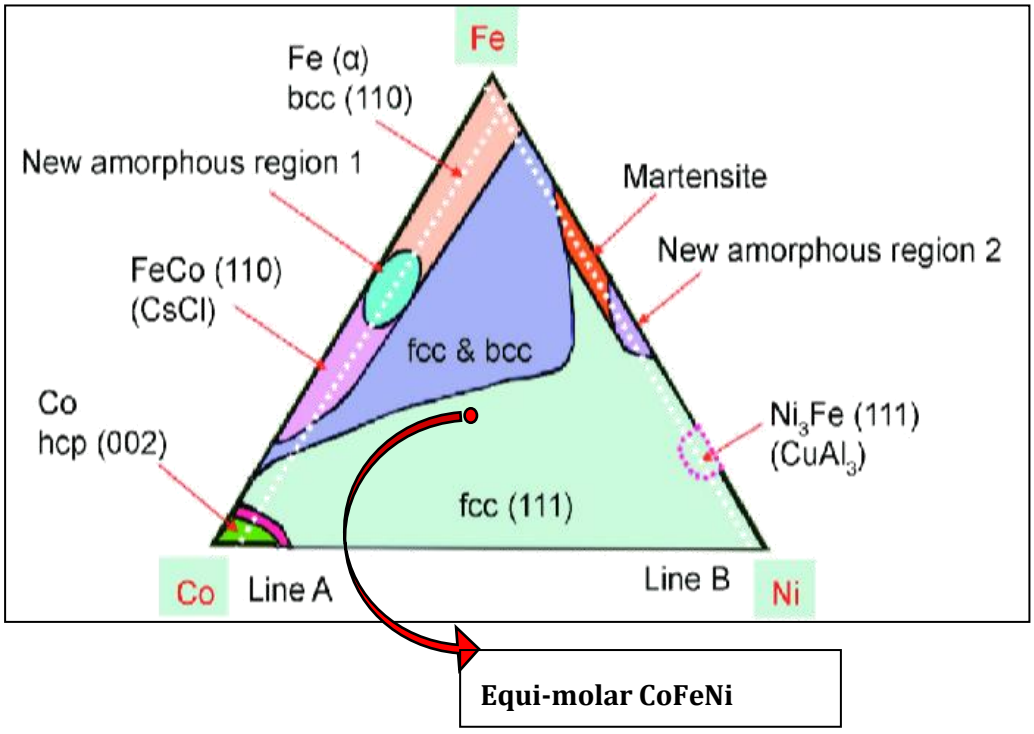

Figure 1. 4: Ternary phase diagram showing equi-atomic amounts of Co , Fe & Ni showing FCC structure[11]

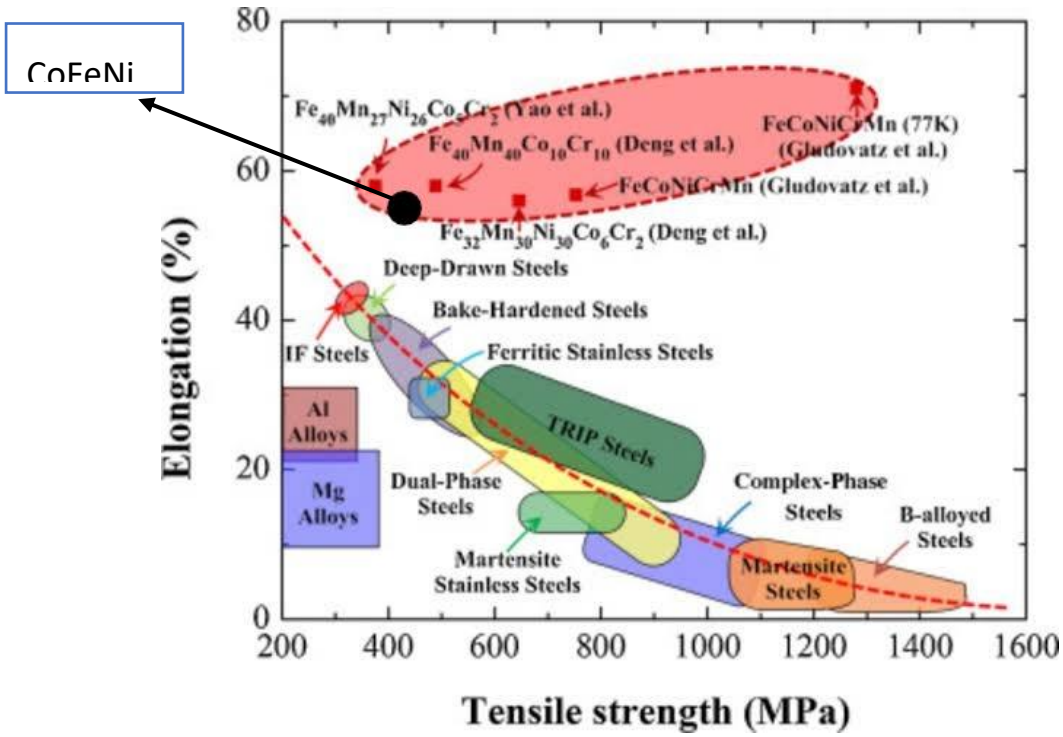

Figure 1. 5: Ashby flow chart for properties comparison [10]

1.2.3 The impact of lattice distortion

Because the component elements' atomic radii differ, substantial lattice distortion occurs in high entropy alloys. The amount of distortion is determined by the sort of atom that occupies the location. The very high increment in configurational entropy observed in HEAs is thought to reduce the intensity of X-ray diffraction peaks in order to increase hardness, reduce electrical and thermal conductivity, and reduce the temperature dependence of these properties due to severe distortion compared to conventional alloys[21]. In high entropy alloys, the words "solvent" and "solute" don't have a traditional meaning. Lattice distortion occurs in high entropy alloys due to variances in the sizes of bound atoms and the varied types of bonding occurring in multiple elements. The characteristics and microstructure of high entropy alloys are both harmed by this type of lattice distortion.

1.2.4 Reinforcements

The matrix has the reinforcing material inserted in it. It provides strength and improved structural and mechanical qualities, but that is not their only function. They can also change physical qualities including wear resistance, friction

coefficient, and thermal conductivity. The reinforcement might be continuous or intermittent. Reinforcement morphology is divided into two categories:

- Continuous Fibres
- Discontinuous Fibres

For continuous reinforcement, monofilament wires and fibres such as carbon fibre and silicon carbide are utilized. The result is an anisotropic system in which the orientation of the material effects its strength since the fibres in a matrix are implanted in a certain direction. Boron filament reinforcements were employed in one of the first MMCs. Whiskers, short fibres, or particles are used in discontinuous reinforcement. The most often used candidates in MMCs are silicon carbide and alumina 155. Discontinuous MMCS may be isotropic and manufactured using typical metal-working procedures like extrusion, rolling and forging.

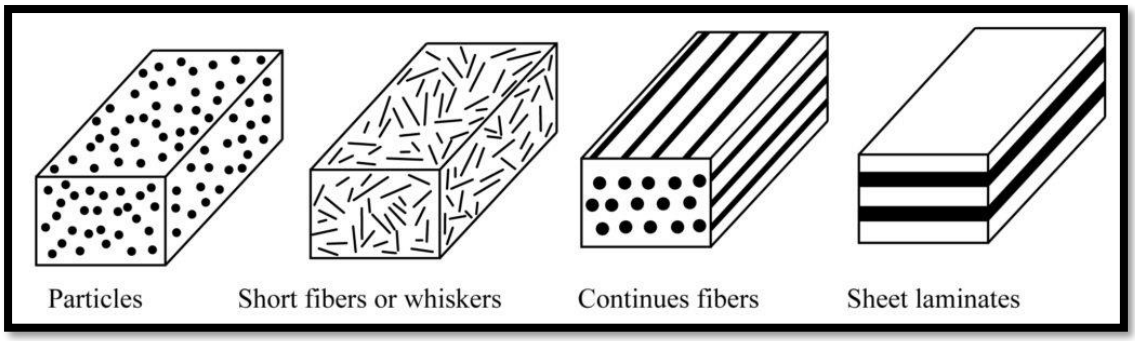

Figure 1. 6 : Type of reinforcement [22]

From a reinforcing standpoint, ceramics are commonly utilised for MMCs because they offer a very desired combination of strength and stiffness at low densities. BN, SIC, ALO1, WC, B4C, TIC, TIB2, graphite, and various other ceramics are among the reinforcing materials with promising futures in the HEA matrix. Furthermore, study on metallic materials as reinforcements, particularly steel and tungsten fibres, has been done. In addition, the shape of the reinforcing material is an important feature in MMCs. For the reasons listed below, reinforcements are an essential component of all composites:

- They provide the matrix material a lot of strength and rigidity.
- They can change the dielectric constant (lower it)
- They have a high temperature resistance and change the coefficients of thermal expansion.

- They increase the material's creep resistance.

The required mix of property and cost usually dictates the choice of reinforcement morphology. Continuous fibre enhanced MMCs are normally the best along the fibre route orientation, but they are also the costliest option. Composites reinforced with chopped fibres and whiskers in aircraft may result in significant improvements in characteristics along the orientation line at lower prices. Because the 03 existing variables of metallic matrix, reinforcement material, and reinforcement morphology are incorporated into the 03 existing variables of reinforcement finding fraction, orientation, composition of matrix, and heat treatments, it is evident that a wide range of material combinations are possible, resulting in a wide range of properties. Powder metallurgy, vapour deposition, diffusion bonding, and liquid metal infiltration under pressure into the preform of the reinforcement are some of the common production procedures utilised to create such composites. The following are the primary aspects that influence the reinforcement's contribution:

- The reinforcement fundamental mechanical characteristic is itself.
- The fibre-matrix surface contact (bond strength) and (the 'interface').
- The percentage of the composite that is reinforced ('reinforcement volume fraction').
- The fibres in the composite's shape (long or short) and orientation (unidirectional, cross-ply, or random).

1.10 Research Objectives

The primary goals of this research project is:

To investigate and improve the strength & ductility combination of CoFeNi by addition of different weight % of WC

1.11 Motivation for Research:

Given that metal matrix composites' noteworthy qualities include adjustable mechanical and thermal properties, there has been minimal research of MMCs

based on homogenous reinforcement distribution, which would have been TERNARY ALLOY. With complicated multi-phase systems, however, a careful balance of chemical affinity and wettability should be difficult to establish. The emerging and pioneering field of Ternary alloy with a near equiatomic composition combining simple single-phase crystal structures with great chemical complexity may provide an answer to this. Ternary alloy are also recommended for applications requiring great thermal and mechanical stability. Ternary alloy are also recommended for applications requiring great thermal and mechanical stability. Considering the advantages and variables that influence the mechanical characteristics of composites, research into such materials is critical for use in aircraft, where improved mechanical qualities are critical. The literature takes a variety of approaches to this, and most of the research are need-based and adapted for a specific goal. It's also true that composite materials used in aerospace applications vary greatly depending on the customer, and there's no formalised collection of manufacturing expertise. As a result, the goal of this project is to examine a variety of innovative TERNARY ALLOY-based composites, select the most cost-effective processing method with an eye toward industrial production, and investigate the materials' uses in aerospace based on the mechanical characteristics found. Project AZM, which focuses on the conceptual design and manufacturing of a fifth-generation fighter jet and a medium altitude long endurance (MALE) unmanned aerial vehicle, was recently initiated by the Pakistan Air Force (UAV (Unmanned Air Vehicle)). Pakistan Aeronautical Complex, Kamra, has built an aviation city and an aviation design institute to accomplish this prestigious goal. This organisation will profit from the concept/development of high entropy composites in the conceptual design and material selection for structural components such as ribs, spars, discs, turbine blades, combustion chamber components, and so on. Furthermore, other strategic organisations can profit from this research and apply the findings to their own structural design areas.

CHAPTER 2

LITERATURE REVIEW

2.1 Ternary Alloy as Matrix

2.1.1 Designing Ternary Alloy for structural applications

A thorough review of the literature advises a focus on HEAs containing Cr, Co, Fe, Cu, Ni, and Mn. They are an extension of austenitic stainless steels, with Ni, Cr, and Fe as the primary constituents. CoCrFeNi occurs in 16 publications, suggesting that these alloys have single-phase FCC microstructures. The following are some of the most important needs and restrictions to consider while building a HEA for aeronautical (structural) applications:

• Because the composition of HEAs varies, the severity of casting flaws may rise. HEAs comprising elements with significantly differing melting temperatures can give a broad range of freezing, which can exacerbate elemental segregation. [95]]

• During mass transport in HEAs, the coordination of the movement of different types of atoms is required, which adds to the difficulty of creating equilibrium phases during casting. [[^{9}6]]

•Density is important, and E is a strength indication. The rule-of-mixtures is expected to offer a realistic estimate of density and E in high entropy alloys. Tm is a symbol for the binding energy between atoms CAA, which is a strength indication and is also connected to the alloy's Tm and T use. Due to its coarse presence, this last criterion contributes in the selection of candidate elements, but it is not intended to be used as a predictive device. We calculate the value of Tm/ p for each element as a statistical rating of palette elements - larger values indicate greater quality.

• According to a rough thermodynamic analysis, AS cont. of high entropy alloys may be sufficient to prevent the production of 5% -10% intermetallic (the ones with lowest enthalpy of formation AH_F^{AxBy} at room temperature). At 1500 K, high entropy alloys can suppress another 30%-55 percent of ordered molecules.

• About half of intermetallic are stable at ambient temperature but unstable at 1500 K, resulting in a unique microstructure control mechanism (through particle dissolution and subsequent precipitation control) and particulate increased HEAs characteristics.

• For a normal solid solution, the mixing enthalpies (AHmix) and enthalpies of formation (AHA) are crucial and must be considered in HEA's stability, in addition to AS conf. In Gibbs-free energies, the strain energy ode is usually neglected, but it is important in the case of HEA. There is currently no quantitative understanding of the strain energy phrase.

•Low-temperature applications (T use 150 °C), medium-temperature applications (T use 450 °C), and high-temperature applications (T use > 1,000 °C) are common HEA systems for structural applications in the energy and transportation domains. A set of physical (density, module) and mechanical (toughness, ductility, and strength) properties is recommended for these three structural HEA classes, To take use of the most efficient reinforcing methods accessible particle hardening, the highest-performing conventional alloys always have a regulated second-phase distribution.

2.1.2 Hume-Rothery Rules

The baseline conditions that determine whether an element may dissolve in a metal and form a solid solution are known as the Hume-Rothery laws. These guidelines are further divided into two groups: one for interstitial solid solutions and another for substitutional solid solutions. The following are the Hume-Rothery rules for substitutional solid solutions:

- The difference in atomic radii between the solvent and solute atoms must be less than 15%.
- To guarantee perfect solubility, the solvent and solute must have identical crystal structures and the solvent and solute must have the same valency.
- The solute and the high-valency metal are predicted to dissolve each other.
- The difference in electronegativities between the solute and the solvent should be low. Because metals have such a wide range of electronegativities, intermetallic compounds can form more easily than solid solutions.

In addition to the modalities, creating a HEA requires high-throughput calculations and tests with a feedback loop for validation; such resources are currently unavailable. 85 percent of the HEAS studied belong to the 3d alloy family of transition metals, with 63 percent having four element branches of CoCrFeNi and 83 percent of the six binary systems in this four-element branch being regular or perfect SS alloys 3). Considering these modalities and the Hume-Rothery laws, we create a HEA matrix with a simple equimolar composition, namely CoCrFeNi.

Because there has been a lot of study done on said HEA, the available data will serve as a yardstick for our HEA matrix production process and will help to validate the manufacture of our unique composite.

2.1.3 Validation of the Ternary alloys matrix design

We completed thorough mathematical calculations to see if our design promises an FCC solid solution after discussing the modalities and needed criteria for HEA design. All the solid solution rules and criteria were validated one by one using analytical calculations, the results of which are listed below:

Mechanical Characteristics

Under 300N load, Aijun Zhang et al.!'°2! calculated the micro hardness (HV) of SPSed CoCrFeNi using an HV-1000 type Vickers's hardness apparatus. The SPSed CoCrFeNi has a microhardness (HV) of 231+23. After imposing a load of 5 kg, a load time of 15 s, and a load rate of 50 m/s, Yih-Farn Kao et al.!('°5Hl estimated microhardness of as-cast CoCrFeNi (produced using vacuum arc melting) to be 116+3 (HV). They also stated that it had an FCC structure with 3.559 A. D. B. Miracle and 4ON grains. [Senkov] Table 2-7 summarises the mechanical characteristics of as-cast CoCrFeNi based on a survey of many publications:

2.2 Particulate Reinforcements

2.2.1 Ternary alloys with WC Reinforcement

Tungsten Carbide (WC) as a reinforcement for High Entropy alloys has received little attention in the literature, according to a review. All the existing research uses a powder metallurgy technique, and no research on WC reinforcement in a

HEA using a liquid processing route has been done yet, which is an unique notion that we are pursuing in our study. The next paragraphs go through the specifics of the available publications.

Rui Zhoua et al [24] investigated the microstructure and wear behaviour of (CoCrFeNi)1x(WC)x HEA-based composites synthesised by spark plasma sintering mechanically alloyed powders. The following are the findings of the study:

• (CoCrFeNi)1-xCWC)x HEA is made up of one FCC HEA matrix phase, one Wrich carbide phase, and one O02 Cr rich carbide phase.

• The length of W-rich carbide is around 4—S5yum. The compositions of Cr-rich carbides are complex, and fine Cr-rich phases can be discovered on a submicron scale.

• Microhardness was tested with a nano-indenter (UNHTL+MCT, Switzerland) under a load of 300 g and 10 mN over a 15-second dwell period. As the loading percentage of WC rises, the hardness of the HEA composite increases continuously, from 603 HV of the (CoCrFeNi)o.07(/(WC)o.03 to 768 HV of the (CoCrFeNi)o.s9(WC)o.11. The HEA composite's strengthening process is caused by the presence of hard WC particles and the precipitation of Cr-rich carbides.

WC was produced and defined by Wenyan Luo and Yunzhong Li.The microstructures and mechanical characteristics of AlCoCrCuFeNi high-entropy alloy composites were examined for effects owing to processing parameters after spark plasma sintering AlCoCrFeCuNi HEA powders were employed as matrix and mechanically alloyed. Following are the findings of the investigation:

• During the procedure, no oxide or other performance-degrading stages were identified.

• The sintered samples' relative densities exceeded 98 percent.

• With increasing HEA matrix content, the HEA matrix showed a notable potential to limit WC grain development and reduce the average size of WC grain.

• With the same processing settings, the average grain size of the WC/HEA composite was 136.5 percent smaller than the WC/Co composite.

• Unlike traditional WC/Co composites, the fracture toughness of WC / HEA composites increases initially with increased Vickers hardness and subsequently declines due to different fracture behaviours caused by HEA matrix suppression of WC grain development.

• After sintering at 1250 °C for 5 minutes with a 10% HEA matrix at a 30 MPa sintering pressure, WC/HEA composites showed good mechanical characteristics. Fracture toughness and Vickers hardness of the composite were determined to be 10. 4IMPa.m!? and 1922 HV30, respectively, which are higher than those of commercial WC/Co composite.

In a 3.5 wt. percent NaCl solution, Liang Weia et al. examined the influence of roughness on pitting and corrosion behaviour of (CoCrFeNi)o s9(WC)o.11 HEA-composite. The EIS and M-S findings revealed that a passive dual-layer film was created on the WC-HEA composite, which increased stability and compactness while reducing roughness.

2.3 Vacuum Arc Melting Process

Christodoulou at al. [1][12] proposed a method for forming composites of discretely scattered second phase particulate matter in a metal matrix made of iron, metallic alloys, or intermetallic, in which the second phase particulate is made of ceramic materials like nitride, carbide, boride, silicon, sulphide, or oxide, or a mixture of intermetallic other than the matrix. Another method involves making intermediate composites with second-phase particles scattered throughout a metallic matrix, mixing the intermediate composites with solid host metal, and using an electric arc to melt the metallic matrix and the host metal, resulting in the dispersion of second-phase particles within the final metallic matrix. Salient points pertaining to our research are appended below:

• Traditional powder metallurgy processes are commonly used to make composites, but the resultant composites are not suitable for remelting due to the

tendency of dispersoid particles to segregate inside the molten metallic matrix, resulting in particle agglomeration after solidification.

• In the molten metal penetration technique, the ceramic material (such as SiC) is crushed to form a compact layer, and liquid metal is poured into the compacted bed to fill the interstices.

• The degassing phase temperature and the extent of applied vacuum are exclusively dictated by the diffusion kinetics and evaporation of any moisture or other gases absorbed[18]. Degassing is aided by high temperatures and low vacuum. In the absence of a degassing phase, the intermediate material generated may be low in density and porous.

• The proportion of second phase particles in the final composite material might vary significantly depending on the intended purpose. For dispersion reinforcement, a second phase particle loading of 1 - 40% volume percent can be utilised. Furthermore, loading fractions of roughly 1 - 10% secondary phase volume can be employed for grain refinement. The intermediate components may have 20 to 80 percent second phase particles, whereas our final composite may contain I to 40 percent second phase particles.

• Contaminants such as oxides obstruct interfacial contact between matrix, layers, and ceramics, reducing composite ductility significantly. These weaker interfacial contacts may result in elongation loss, decreased strength, and quicker fracture propagation.

2.4 Conclusion of the Chapter

Considering the above, we decided on CoCrFeNi as the final composition of our HEA matrix, which was confirmed using Hume Rothery rules and solid solution requirements for HEA, as summarised in Table 2-8:

The design factors for selecting candidates for reinforcement in the HEA matrix are high stiffness, high young's modulus, and high compressive strength. Ceramic reinforcements have these properties in abundance. SiC, WC, BN, and AlzO3 have been chosen as reinforcements to be introduced into the CoCrFeNi matrix for the fabrication of four distinct composites. "Particulate reinforcement" was chosen as

the morphology. We learned in the previous chapter that the morphology of the reinforcement is determined by the desired property/cost combination. Particulates give a more modest but isotropic improvement in characteristics and are often the most affordable option. According to the literature, the loading fraction would range from 5 to 20% by weight.

Because MMCs synthesised by conventional powder metallurgy techniques are typically unsuitable for remelting due to the tendency for the dispersoid particles to segregate within the molten matrix metal, causing particle agglomeration upon solidification, the processing route chosen after reviewing the literature is vacuum arc melting. Furthermore, we discovered that in the powder metallurgy approach, there is a significant possibility of impurities such as oxides, which prevent interfacial interaction between the matrix and the ceramic phase, lowering the composite's ductility [30]. Reduced strength, elongation loss, and fracture propagation can all occur from a decreased interfacial contact. Vacuum arc furnaces, on the other hand, are pollution-free and provide excellent metallurgical control. Another advantage is the flexibility of vacuum arc furnaces, which can be started and stopped quickly.

The publicly reported data discussed in this chapter will be used to evaluate and validate our technique, as well as future microstructure, crystal structure, and mechanical characterizations.

CHAPTER 3

EXPERIMENTAL TECHNIQUES

As discussed in chapter 2, the ternary alloy matrix for composite system in this research work is CoFeNi. 3 different systems are synthesized and analysed incorporating WC reinforcement in different weight percentage. The synthesis route opted is liquid processing via vacuum arc re-melting equipment. The microstructures have been identified through polarized optical microscopy and scanning electron microscopy (SEM) while the compositions have been verified through energy dispersive spectroscopy (EDS). Furthermore, the composition of phases has been identified through x-ray diffraction (XRD). All the samples were subjected to mechanical testing which included micro & macro hardness and compression testing. The various steps involved from preparation of alloys till its characterization are as follows: -

- Compositional estimations & calculations
- Composite synthesis via vacuum arc melting
- EDM (wire) Cutting of Samples
- Metallographic Analysis
- Microstructural and crystal structure characterization
- Mechanical characterization

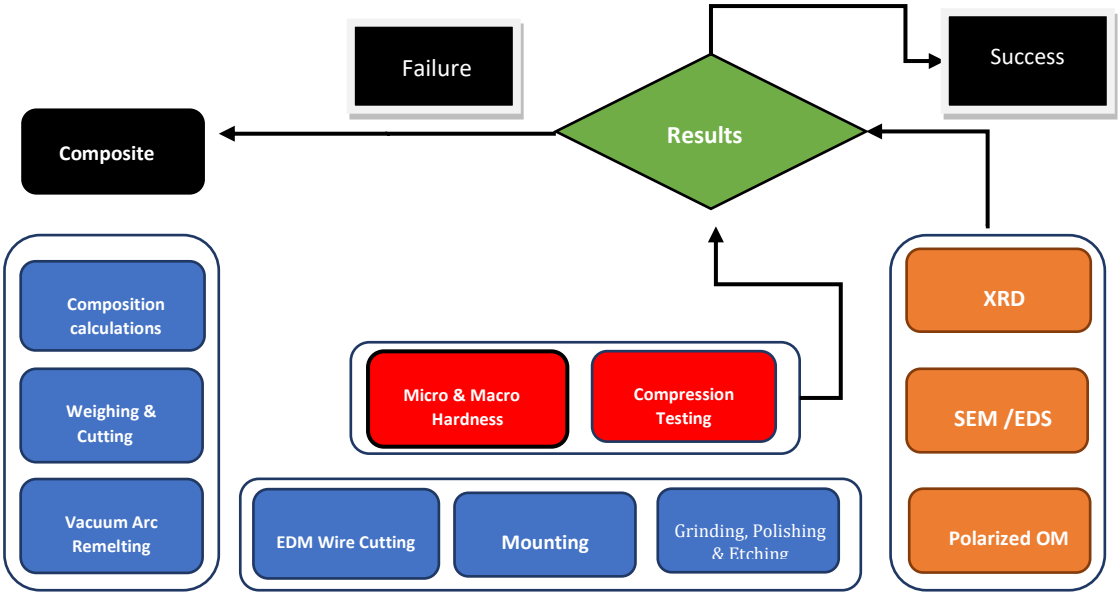

Figure 3.1: Schematic flowchart of all the processes involved in the experiments

3.1 Synthesis

The synthesis of ternary alloy-based composite was done in a two-shot process:

- Synthesis of ternary base alloy matrix i.e., CoFeNi
- Remelting of alloy over the preform of WC reinforcement powder in different weight percentage

3.1.1 Compositional calculations

The purity of the starting material is also very critical as minute amounts of foreign components can make a significant difference in the tests. High purity metal powders (99.95 %) were therefore used for the present study as the starting materials. For the base ternary alloy matrix, equimolar concentrations of pure metals (Co, Fe, Ni) were considered, and associated weights percentages were calculated utilizing the following:

formulae:

$$\boldsymbol{Weight\ of\ X\ \ at.\%\ atom}s = \frac{(At.\%)(Atomic\ weight)}{Avogadro`s\ Number}$$

$$\boldsymbol{Wt.\%\ of\ X} = \frac{(\boldsymbol{weight\ of\ X\ \ at.\%\ atoms})}{\boldsymbol{Total\ weight\ of\ all\ constituents}} \times 1($$

Conclusively, following weights of each element in each of compositions were finalized:

Table 3. 1: Calculated elemental weights of finalized compositions

SAMPLE COMPOSITION	Final Wt. (g)	ELEMENTAL Wt. (g) @ 33.33% atomic wt.				Reinforcement WC Wt..	
		Co	Fe	Ni	Total wt.	wt. %	wt. (g)
CoFeNi- 0 wt. % WC	25.0011	8.4923	8.0483	8.4605	25.0011	-	-
CoFeNi- 1.0 wt. % WC	25.3772	8.4928	8.0485	8.4607	25.0020	1.0	0.2501
CoFeNi- 2 wt. % WC	25.5030	8.4927	8.0488	8.4607	25.0022	2	0.5008

3.1.2 Sample Preparation

Samples of desired composition were prepared by mixing the equimolar amount of pure metal pieces (Co,Fe and Ni) by first cutting and then weighing to match the calculated weights and stored separately to ensure purity and uniformity. WC powder was also weighed separately and stored separately. The metallic pieces were then subjected to melting under argon atmosphere. The electric arc furnace was used for melting given the high melting point of constituent elements. The schematic and photograph of the electric arc furnace used for sample preparation during this analysis is shown in the following figures:

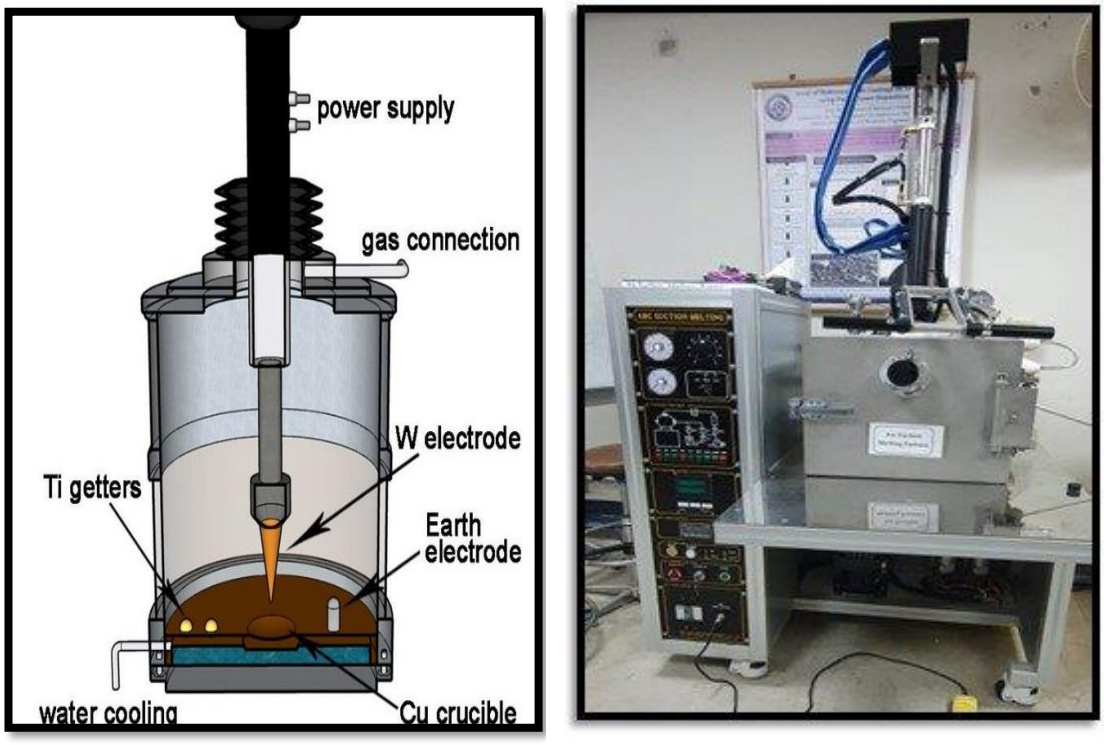

Figure 3.2: (left) Schematic of a typical Vacuum Arc Suction Remelting (VAS) furnace; (right)Vacuum Arc Suction furnace present at Alloy design Lab SCME- NUST

As illustrated in the figures above, the electric arc furnace used during present study consists of a non-consumable tungsten electrode serving as a cathode and a water-cooled crucible that acts as a sample holder and as part of the anode.

The pieces to be melted were put in the copper crucible for the alloy preparation, the furnace chamber was closed, and a secondary vacuum of 2 x 10^{-5} bar was introduced to eliminate atmospheric gasses that may cause oxidation during the melting process. Once the necessary vacuum value was achieved, high purity argon gas was introduced into the chamber to prevent the evaporation of

components with high vapor pressure, i.e., Ni in current research work, during melting. The insertion of the argon into the chamber also eased the movement of the tungsten electrode and the electric arc. Arc was then struck on the charge by moving the tungsten electrode towards the copper platform. As soon as the arc was struck, a current of high intensity appeared which ionized the argon atoms present in the furnace chamber. The electrode was then moved towards the titanium getter, which upon melting ensured that no free oxygen was left in the furnace chamber. The electrode was subsequently moved towards the metallic pieces, which behaved like a counter electrode in contact with the copper crucible, and as a result, strong current passed through them. A few seconds later, the pieces were melted. Upon melting, the electrode was finally moved to the crucible's border and the arch was switched off. The final shape of alloys after melting was spherical buttons as shown in Figure 3-3:

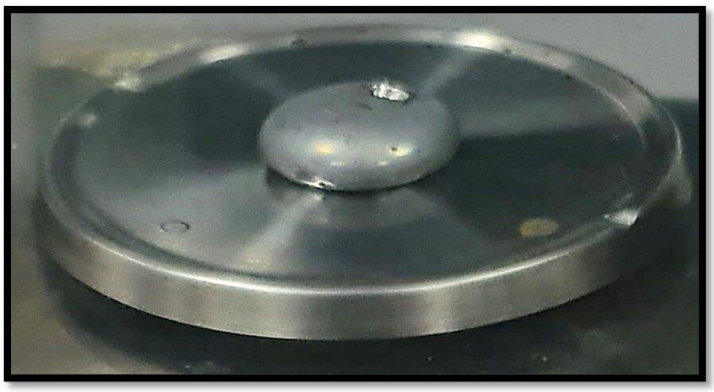

Figure 3.3: Melted ingot from Vacuum arc melting furnace

The melted alloys should have a homogenous composition because the macro inhomogeneity left during melting are difficult to remove later. Therefore, to achieve a homogenous distribution of the constituent elements in the alloys, the alloys were flipped over after melting and melted again. To achieve maximum homogeneity, this process was repeated 4-5 times forming ternary alloy. The weight of each specimen was calculated before and after melting to keep a record of weight loss during the preparation of the sample. In m cases, there was even less than 0.5 percent weight loss during melting.

Then samples were again placed in the crucibles and then WC powder of weight % 1.0 and 2.0 was placed at one side of crucible and again subjected to vacuum and melted. WC powder placed at one side of crucible was done so that first

ternary alloy shall be melted by the arc and arc shall not cause any sputtering in the samples. As soon as the alloy melts again the powder got mixed in the solution. Then arc was circulated in the melt to ensure uniform mixing and dispersion of WC in the metal matrix to achieve homogeneous properties throughout composite. The first melting cycle ensures mixing and rest 4 were aimed for the same purpose as mentioned above. The weight addition was calculated by weigh balance to confirm the amount of powder addition in the alloy samples.

The VAM furnace available at SCME, NUST is suitable for small samples about 25 grams. In the case of large specimens, large surface area of the specimen would be in contact with the water-cooled copper crucible and as a result, full pieces melting can be difficult, which can induce inhomogeneity. The weight of the composite sample was around 25 grams.

3.1.2 EDM Wire Cutting

After the sample synthesis through vacuum arc furnace, the samples were outsourced for Electrical Discharge Machining (EDM) or also called Spark Machining to cut out samples for different characterizations and mechanical testing according to different dimensions.

6 samples were cut off for Compression Testing according to ASTM E9 standard having dimensions 3 ×3×7mm as cylindrical samples are required by this standard for Compression testing. 1 sample was cut out for XRD characterization measuring 0.85-0.9 mm in thickness according to machine limitation for the bulk samples. 1 sample was cut out for Polarized Optical Microscopy & SEM and same sample was used further for Micro and Macro Vickers hardness testing.

3.2 Metallography

After performing heat treatment on the samples metallographic examination of samples was done. Steps involved in metallographic examination of samples consist of

- Mounting
- Grinding
- Polishing

- Etching
- Polarized Optical Microscopy
- Structural Characterization (Optical Microscopy and SEM)

3.2.1 Mounting

Mounting of samples was done by using Bakelite powder. During mounting samples were compressed and heated in presence of Bakelite power so that they form a solid disk to facilitate ease of handling samples during subsequent grinding and polishing. Temperature and pressure were set at 180°C and 280 bar respectively.

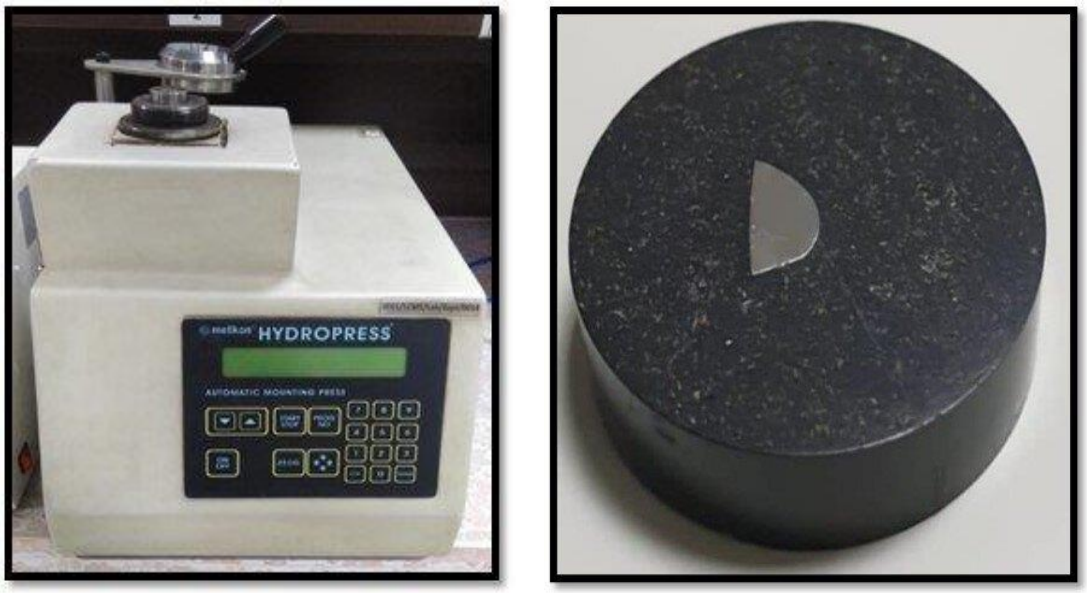

Figure 3. 4: (left) Mounting press in SCME, NUST (right) Mounted specimen

3.2.2 Grinding

Most metallurgical features are microscopic in size; when viewing through light microscopes, they cannot be visualized without at least 50x to 1000x magnification. A metallic specimen must be ground and then polished to a very fine mirror like finish to examine these features.

Figure 3.5: Grinder / Polisher in SCME, NUST

Grinding of samples was done by using standard grid size silicon carbide papers. Grinding was started from 600p grit size till 200p grit size paper for short time period and slower speeds for lower grades emery paper as having high abrasive effect to sample and to eradicate the chances of formation of deep scratches due to high abrasion effect that cannot be eliminated by next grade paper and forms issue in polishing stage of metallography .Higher grades emery papers employ high speeds and more time for grinding as lesser abrasion effect of these papers which require higher speeds and higher times The directional change of 90° after each emery paper was ensured. Optical microscope was used to confirm elimination of envious scratches and formation of new ones with each emery paper.

Table 3. 2: Different grade emery papers with speeds and operation time

Emery paper grade (SiC)	Time of Grinding	Speed (rpm)
600p	30 sec	350
800p	1 min	350
1000p	1 min 30 sec	400
1200p	2 min	400
1500p	2 min 30 sec	500
2000p	3 min	600

3.2.3 Polishing

After grinding of samples, the final surface finish was achieved by polishing the samples. Polishing of samples was done by using multiple media i.e., 0.5 & 1-micron alumina suspension and 0.3, 0.6 and 1-micron sized diamond paste with NYLON pad for intermediate polishing and RYON for very fine polish (mentioned in table). Different media were employed as Alumina suspension couldn't achieve finishing required for proper characterization as scratches weren't resolving so Diamond paste was acquired and utilized for polishing purpose which resulted in proper finishing and resolution of fine scratches on surface of specimen. The results were confirmed through optical microscope.

Table 3. 3: Different Polishing media with matte types and operation speed

Polishing time	Matte type	Speed (rpm)
Alumina suspension 1µ particle size 0.5µ particle size	METKON 1.0µ size polishing pad	350 600
Diamond paste 0.6µ, 0,3 & 0.1µ particle size	METKON 1.0µ & 0.5µ size polishing pad	600

3.2.4 Etching

Unfortunately, the polished surface under a microscope looks identical to a flashy white field. Metallographic etching is a chemical process which reveals the microscopic features of metals. The physical properties and performance failures of a specific metal sample can be determined and explained by analysing the quantity, character, and distribution of these various characteristics [1][13].

Etchants are the chemical solutions that create such a contrast between component of the microstructure. They selectively corrode the high energy areas like grain boundaries which shows up as darker regions owing to the differences in the composition, structure, or phase of metal which have different rates of corrosion upon chemical interaction with an etchant. Etching therefore exposes" [1][13]:

- The size and shape of grain boundaries (defects in crystal structure)
- Different phases (different types of compositions / crystal structures in an alloy)
- Inclusions or contaminations (small amounts of non-metal material)

Aqua regia was applied first but sample wasn't etched properly, and difficulty was faced in distinguishing microstructure, so another reagent Kaling's agent was used and tested for different times as first attempt over etched sample at 8 sec. The samples were etched for 6 sec from this medium.

Table 3. 4: Different Etching media with etching time and compositions

Etchant	Etching time	Composition
Aqua regia (HCl: HNO_3)	8 sec per sample	3: 1
Kaling's Agent (HCl: Ethanol-$CuCl_2$)	6 / 8 sec per sample	100 ml HCl -100 ml ethanol -5 g $CuCl_2$

3.3 Characterization Techniques

3.3.1 Polarized Optical Microscopy (OM)

In this technique, the specimens invisible due to optical anisotropic behaviour of their surface are make visible by utilizing the polarization of the light in Monocular Polarized Light Optical Microscope. this is done by having contrast when light interacts with double refracting surface producing different patterns when reflected from surface of specimen as result of constructive and destructive interference giving different colours and intensity in image seen through camera placed and recorded in computer at back [34].

Images at different resolutions were taken from different parts of sample to look for microstructure etched from different media to detect which etchant is best fit for use and which reveals proper grain boundaries and grains in microstructure.

.

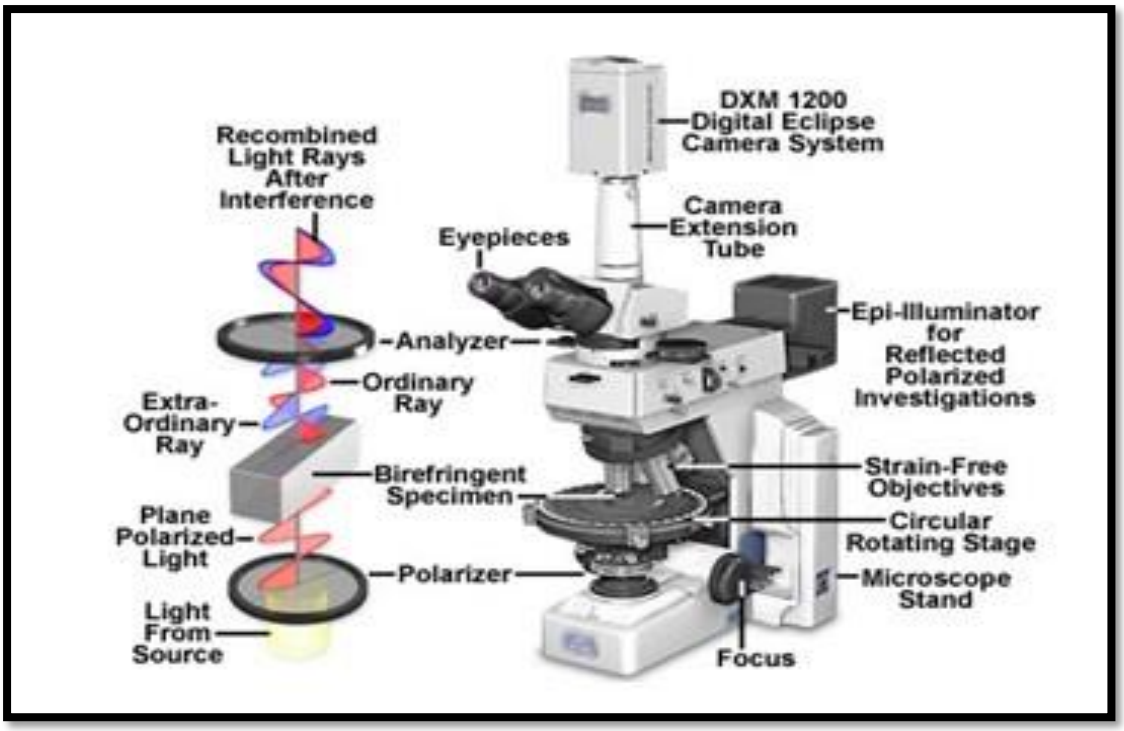

Figure 3.6: Schematic of Polarized Optical microscope

3.3.2 Grain Size measurement using IMAGE J software

The Grain size of the image acquired from Polarized light Optical microscopy was done using Image J software. This was done by using Linear Intercept method by drawing equal length lines at different sections of image taken at fixed resolution for all specimens and then looking out for grain boundaries and number of grains cut by line and then dividing by absolute length of line[40].

Figure 3.7: Linear Intercept method applied ion OM images for Grain size measurement

3.3.3 Scanning electron microscope (SEM)

In this technique, the fine beam of electrons is focused over a specimen's surface. Photons or electrons are knocked off from the material's surface in the result. These knocked off electrons are then focused on the detector. The output from the detect0r modulates the brightness of the cathode ray tube (CRT)[1][14]. For every point where the electron beams are focused and interact, it is plotted on consequent point on CRT (Cathode Ray Tube) and the material's image is produced

The electron-surface interaction causes the release of secondary electrons (SE), backscattered electrons (BSE) and X-rays [1][15]. Common SEM mode for detection is via secondary electrons. These electrons are emitted from near the sample surface.[38] So, a pronounced and clear image of the sample is obtained. It can reveal sample detail even less than Inm in size. Also, elastic scattering of incident electrons also takes place and release back scattered electrons. They emerge from deeper locations as compared to secondary electrons. So, their resolution is comparatively low. When an inner shell electron knocks off from its shell it emits characteristic x-rays[1][16].

SEM was done to figure our sample's morphology, crystallography, and orientation of planes. Magnification of SEM can be controlled from 10 to 500,000 times. Morphology of the materials were examined on (JEOL-JSM- 6490LA) along with Point and Area analysis and EDS to look for unform distribution of particles and constituents in the structure which was our aim for this processing route and fabrication.

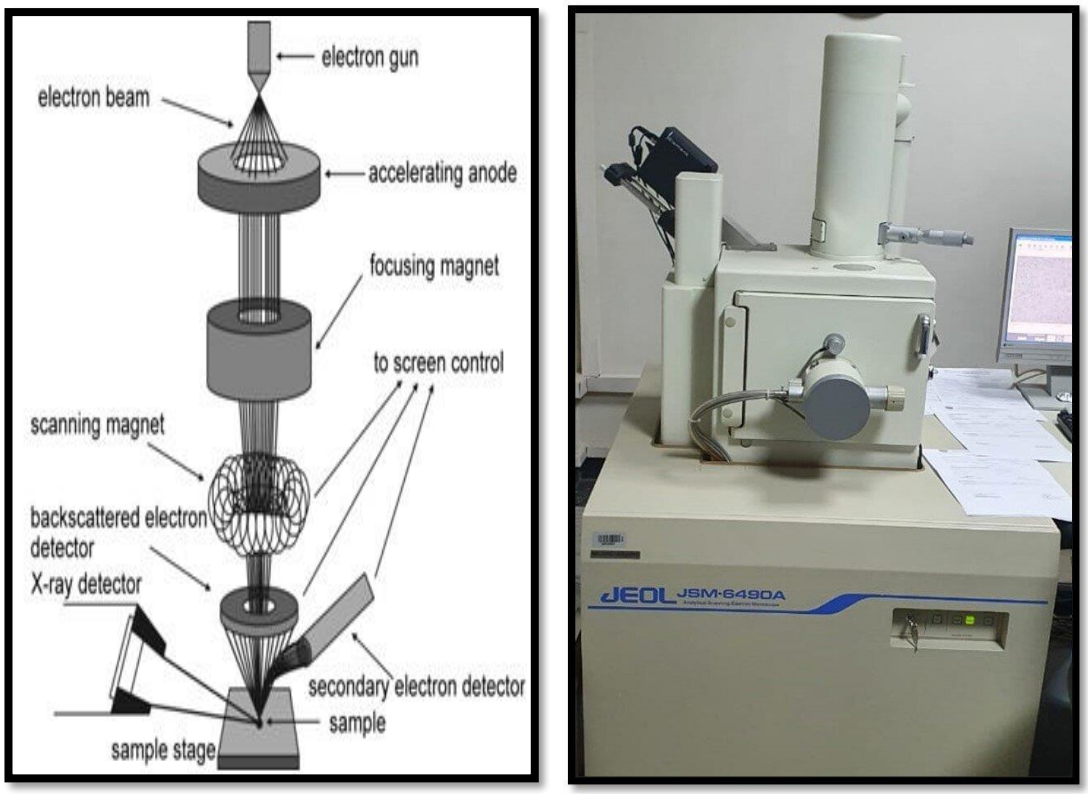

Figure 3.8: (left) Schematic of SEM; (right) JOEL JSM-6490A PRESENT at SCME

3.3.4 Energy Dispersive Spectroscopy (EDS)

Elemental composition was determined by EDAX (EDS) detector attached to **JOEL JSM-6490A** at SCME- NUST, which allows to perform elemental analysis of a sample by means of analysis of the characteristic x-ray spectra. The characteristic x-ray spectrum is one of the products of interaction between electrons and atoms of the observed specimen.[41] This helped us get the elemental composition at different points on each of the visible phases in the samples as well as the line scans of area of interest. The parameters set for the EDS analysis were as follows:

Table 3. 5: EDS Parameters set during scans

Parametres	Value
Working Distance	15 mm
Voltage	20kV

3.3.5 X-rays diffraction (XRD)

X-rays diffraction (XRD) analysis was used for identifying phases and crystal structure determination of the developed materials. It is a non-destructive method

and provides fingerprints of Bragg's reflections of crystalline materials [1][17] XRD is most common in studying crystal structures and atomic spacing in crystalline materials. The basic principle of XRD is the interference of monochromatic X-rays produced in the cathode ray tube. The monochromatic concentrated x-rays are then directed towards the sample. These rays interact with the sample and constructive interference occurs where Bragg's law satisfies. The diffracted x-rays from the sample are detected and counted by detector. All directions of diffraction from lattice can be achieved by scanning the sample up to 20 range. Diffraction peaks in XRD can be used to calculate the d spacing. As every phase has unique d-spacing so it can be used to identify phases in crystalline materials.

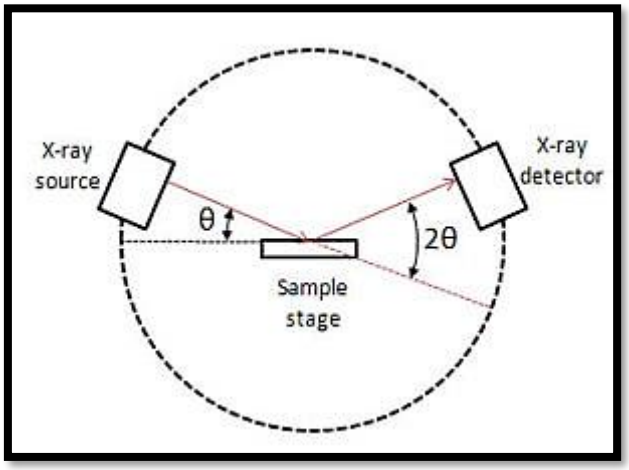

Figure 3.9: XRD Schematic

It consists of 3 main parts. A cathode tube, sample holder and x-ray detector. X. rays are produced by heating filament element which accelerates electrons towards a target which collide with target material with electrons. Crystal is composed of layers and planes, x-ray which hay wavelength like these planes is reflected such that the angle of incidence is equal to the angle of reflection. "Diffraction" takes place, and it can be described as by Bragg's Law below; where d is interplanar distance of scattered rays, n is a positive integer related to order of reflection, X is the wavelength of incident rays and 0 is the scattered angle[34].

$$2d \sin \theta = n\lambda$$

When Bragg's law is satisfied, constructive interference takes place, and "Bragg's reflections" will be picked up by the detector. These reflections positions tell us about inter-layer spacing-ray diffraction tells us about the phase, crystallinity, and sample purity. By this technique, one can also determine lattice mismatch, dislocations, and unit cell dimensions.

Figure 3.10: BRUKER D2 PHASER XRD setup at SCME- NUST

X-ray diffractions were performed by BRUKER D2 PHASER XRD diffractometer at SCME-NUST by carrying firstly the full scan of the sample to look out for the peaks of CoFeNi as being a FCC phase and WC particles peak, Unfortunately , due to lower amount of WC addition in the matrix the peak of WC appeared in the result when plot was indexed by the software of the machine but its intensity was wo low that it got removed in noise reduction . Slow angle scan was done for the specimen (the parameters mentioned below) within angular range known from reference XRD plot of WC as to gain better clarity of the specimen and to achieve WC peaks in sample which determines that WC has not formed a phase but retains its identity as needed by composite constituents' elements[45].

Following parameters were set during each scan:

Table 3. 6: XRD Parameters set during scans

Parametres	Value
Full Angle Scan	
Scan Angle	20˚ - 80˚
Step size	20kV
Scan rate	1 sec/ step
Scan time	90 min
Slow Scan	
Scan Angle	30˚ - 45˚
Step size	20kV
Scan rate	1 sec/ step
Scan time	90 min

3.4 Mechanical testing

3.4.1 Hardness Test

Micro & Macro hardness tests were performed to measure the hardness or resistance to penetration of small or thin samples. Results of hardness test provide information about surface features of components and case hardness and case depths of carburized parts can be determined precisely.

Vickers (DPH) or Knoop diamond indenter is used to measure the hardness of materials. Load up to 1000g applied on indenter causes the plastic deformation in the surface of' material. The shape of indentation is according to the shape of indenter. Both tests (Vickers and Knoop) require accurate measurement from indent on the surface material; these values are then put into the formula to calculate the hardness of materials. Micro hardness microscope is used to measure dimensions of indent because the size of indent is very small. Although macro hardness test has larger indent but to calculate the dimensions of sample

microscope with the apparatus is used and the dimensions are fed into formula to find hardness.

In Knoop hardness test rhombus shape indenter is used to calculate the hardness. It involves applying force of 1000 g or less for certain amount of time. Application of force causes indenter to penetrate the surface of sample. Depth of penetration is used to calculate the hardness of material. Hardness value on Knoop scale is based on load and measurement of indent on the surface of sample.

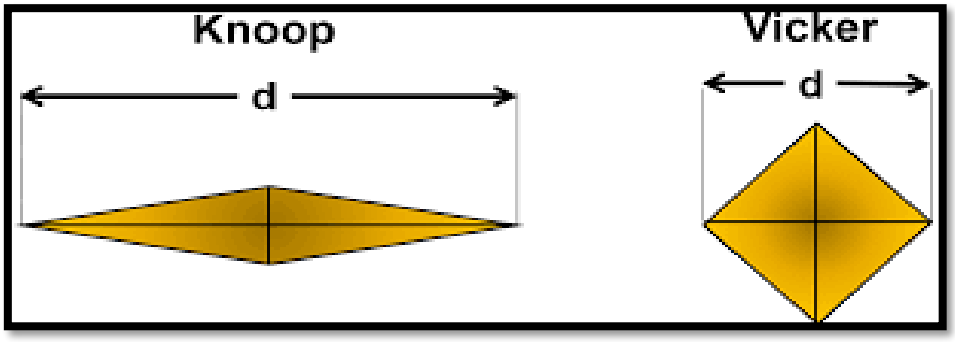

Figure 3.11: Knoop and Vickers indenters

In Vickers hardness test pyramid shaped diamond indenter is used to measure hardness of materials. Vickers hardness test is applicable to both micro and macro scales. Like Knoop hardness test, in Vickers test load is applied on the sample for certain period. Application of load for certain time produces indent in the sample, length of diagonal of indent is measure with the help of microscope. Putting the values of load and length of diagonals in the formula gives the hardness of materials. [9][11] . Micro hardness is found for lesser loads and greater precision as it covers very small area under indent and macro hardness is for larger indents covering large area under the indent.

$$\mathrm{HV} = 1.854 \times \frac{F}{D^2}$$

Where F : Applied major load on specimen (measured in kilograms- force)

D: Area of Indentation (measured in millimetre square)

For macro hardness indent was placed and diagonals values were measured and by relating the values of indent diagonal with the machine manual hardness values were found. The purpose of doing both tests was to check the precision of results and to ensure that WC is uniformly distributed not present in segregated from in the matrix.

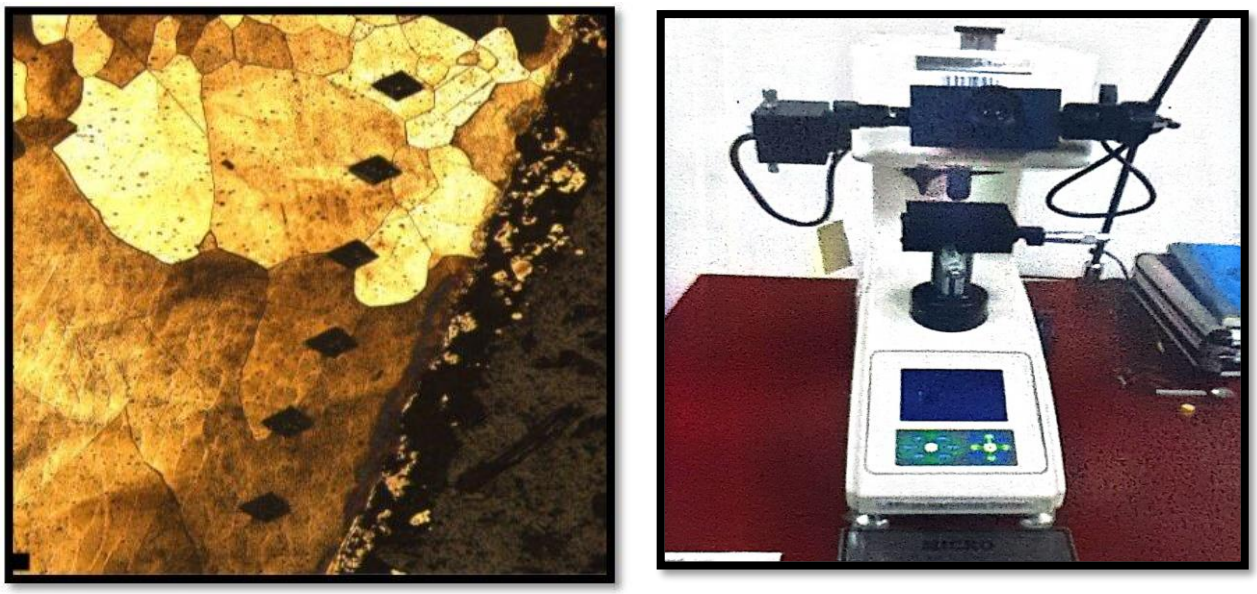

Figure 3.12:(left) Microhardness indents (right)Micro Vickers hardness tester at SCME, NUST

The specimen was tested under different load (mentioned in table) for different times at different regions of samples and average was taken to see the relation between results and to predict the hardness values of sample.

Table 3. 7: Hardness parameters set during testing for different apparatus

Vickers Hardness type	Dwell Time	No. of Indent per sample	Load
Micro Hardness	10 sec per indent	~10	0.5 kgf 5N
Micro Hardness	10 sec per indent	~3	30 kgf 300 N

3.4.2 Compression Testing

The compression test is carried out on materials to ascertain their behaviour under compressive loading by determining mechanical properties' parameters like yield strength, elastic limit, elastic modulus, ultimate compressive strength.

By analysing these parameters, it can be established if the designed material is suited for the intended application or if it will fail under them.

Compression testing for alloys is conducted on universal testing machine (UTM) with flat plate fixtures. The SHIMADZU UTM at SCME was utilized for this purpose. From the literature, the value for strain rate was set at I x 10^{-3} sec .

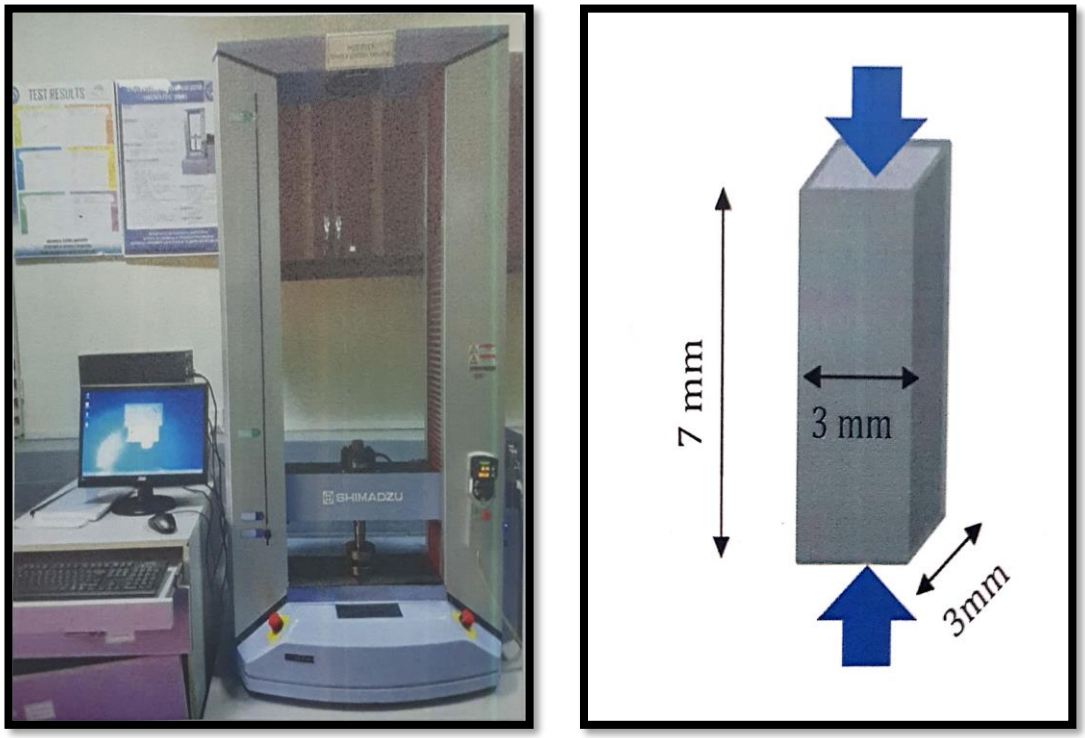

Figure 3.13: (left) SHIMADZU Universal Testing Machine (UTM) at SCME, NUST (right)Specimen for compression testing

For the specifications of testing specimen, ASTM E9 standard was consulted and the specimen with following geometry and dimensions were made through EDM (wire) cutting of ingots.

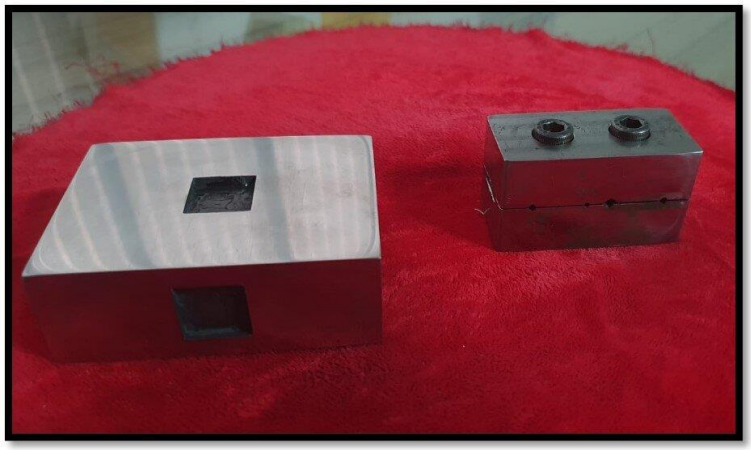

Figure 3.14:(left) Die for Specimen preparation

The most common impediment faced during compression testing of such slender specimen is buckling that is characterized is a material failure where unstable lateral deformation of specimen takes place under compressive forces. These failures are a result of either non-uniform force distribution over the cross-section surfaces or due to local inelastic instability over the columnar length of the material. Carbide inserts were therefore placed above & beneath the specimen to ensure uniform force distribution over the cross-sectional surfaces and avoid buckling, as shown in Figure 3-15:

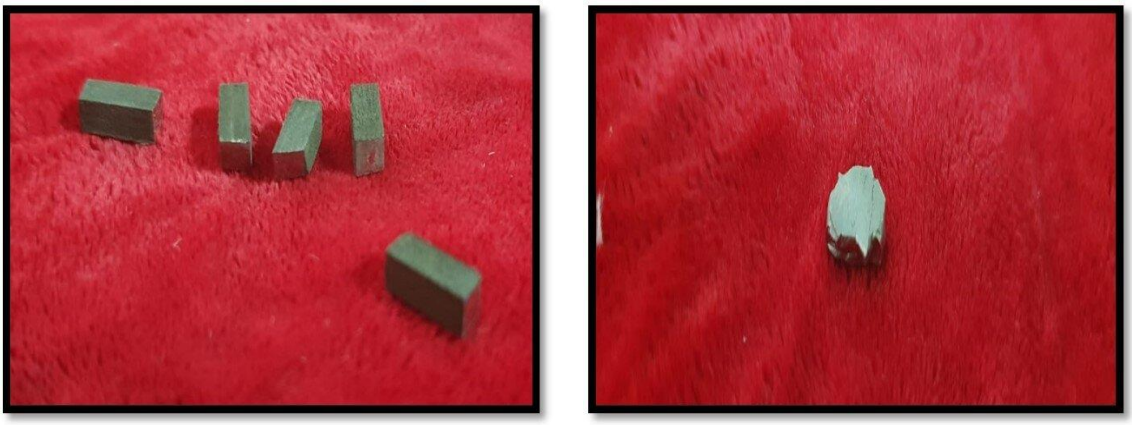

Figure 3. 15: Specimen before (left) and after (right) compression testing.

To make the results more meaningful, 03 specimen per system were tested and the results were averaged out. It is important to know here that ductile samples tend to exhibit sharp kneed stress-strain curve with distinct yield point however, the brittle samples may be tested to failure as they would break either by shattering or crushing. The broken pieces may act as an unguided shrapnel fired around therefore care must be taken by surrounding the test area with a protective material.

3.5 Conclusion of the chapter

The characterization techniques were studied and finalized for our research. The microstructure characterization of synthesized systems was done through Polarized light optical microscopy, scanning electron microscopy (SEM) and energy dispersive spectrometry (EDS) while the crystal structure characterization had been done through X-ray diffraction (XRD). Based on the characterization

results, the system was further studied with varying loading fraction of the WC reinforcement and subsequently mechanic testing was conducted upon them. The mechanical testing includes micro & macro hardness and compression testing.

CHAPTER4

RESULTS AND DISCUSSIONS

Scanning Electron Microscope (SEM) and Optical Microscope (OM) was used to evaluate the microstructures of samples after the synthesis of in as-cast structures. The purpose of SEM was to observe how well the alloy was synthesized through correlation with existing literature. On the acquired samples, EDS analysis was done to evaluate the compositional profiles through point and line spectrums. Furthermore, the evaluation of the of microstructure with the addition of different weight percent of tungsten carbide was the object purpose. All the samples for microstructural characterization were grinded and polished by using standard metallographic procedure. The samples were then etched with kalling agent with composition 100 HCL, 100 ethanol and 5-gram $CuCl_2$ to reveal the grain boundaries.

4.1 AHM-1 (CoFeNi – Matrix)

The first ternary alloy-based composite synthesized is designated as AHM-1 which comprises of pure CoFeNi and no added WC as reinforcement.

4.1.1 Microstructure Characterization

SEM and OM micrographs and the associated EDS analysis of ternary alloy i.e., CoFeNi in as-cast condition are shown in 4-1:

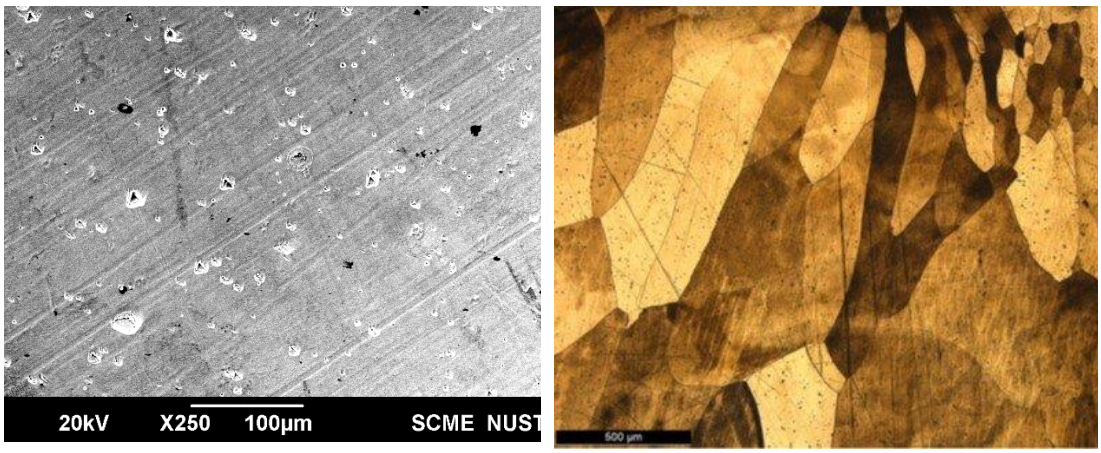

Figure 4. 1: (Left) SEM micrograph of Ternary Alloy Matrix (as-cast CoFeNi); (Right) Optical micrograph

Table 4. 4: Elemental composition AHM 1(at.0 % WC) from EDS

EDS Analysis of CoFeNi-0 wt.% WC		
Element	**Weight %**	**Atomic %**
Fe K	33.3	34.4
Co K	34.1	33.5
Ni K	32.6	32.1

The microstructural characterization through SEM revealed a single-phase microstructure uniformly distributed50. From EDS analysis, a uniform distribution and equimolar elemental composition was revealed.

4.1.2 Crystal Structure Characterization

The sample was scanned from 20-80 degrees for 90 minutes. During crystal structure characterization through XRD, these results were obtained in which the peaks are typically of FCC crystal structure which confirms its formation. The results are fully coherent with the available literature.

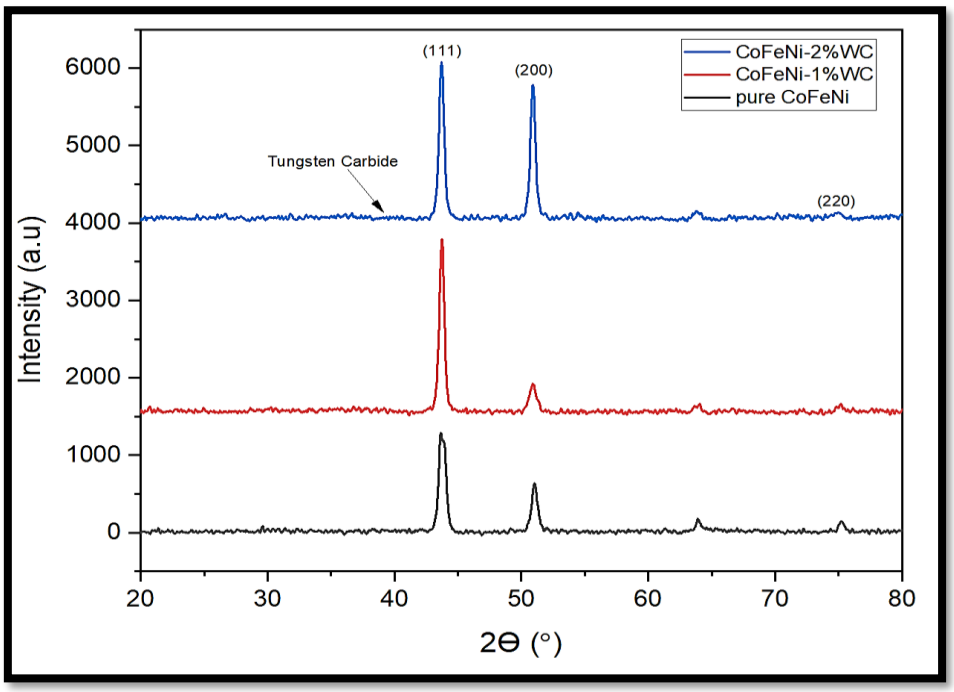

Figure 4. 2: XRD plot of Ternary Alloy Matrix (as-cast CoFeNi, as-cast CoFeNi + 1wt.% WC, as-cast CoFeNi + 2wt.% WC)

4.1.3 Mechanical Characterization

Micro-Vickers Hardness (HV) testing was done under the action of 5N load with a dwell time of 10 seconds. The obtained average value was 117.9 ± 5 HV., showing that the ternary alloy is soft and ductile. It could not be compared with a reported value due to the difference in parameters of the test.

Macro-Vickers Hardness (HV) was done in which the load was 300 N, and the dwell time was the same as Micro-Vickers hardness i.e., 10 seconds. The value of hardness obtained from this test was 121.8 ± 5 HV that was coherent to the result of Micro-Vickers hardness test.

Compression Testing was performed with SHIMADZU UTM at SCME, NUST under the strain rate of 1 × 10-3 m/sec. Carbide inserts above and beneath the specimen and 01 specimen was tested. The yield strength obtained was 115.7 ± 4 N/mm^2. This value could not be compared to the value in the literature as that value was obtained from a tensile test and cannot be compared to a compression test value.

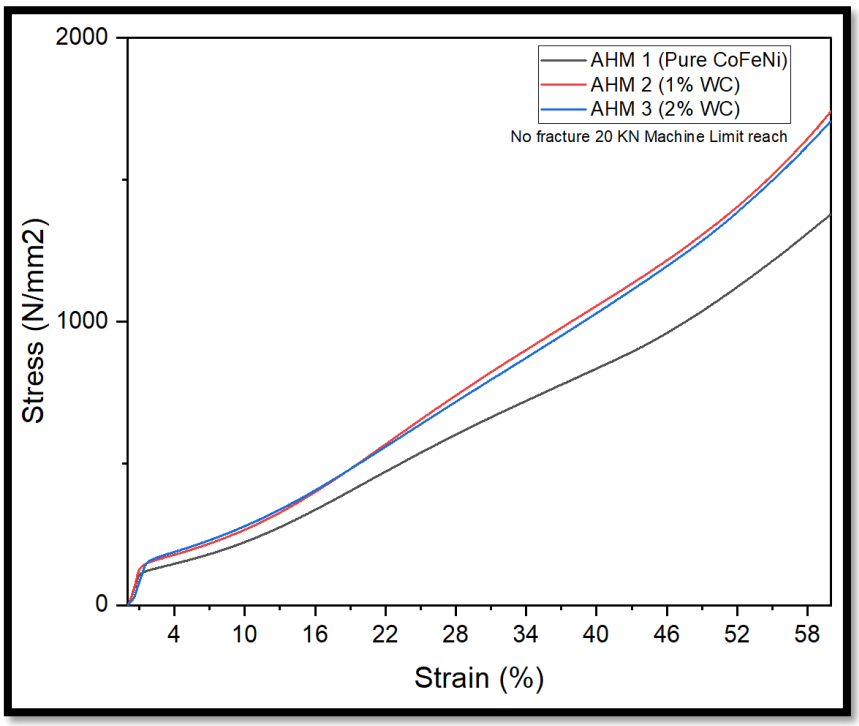

Figure 4. 3: Stress-Strain curve of AHM-1 (as-cast CoFeNi, as-cast CoFeNi + 1wt.% WC, as-cast CoFeNi + 2wt.% WC)

From the stress-strain curve obtained through compression testing, the ternary alloy matrix (as-cast CoFeNi) is found to be highly ductile and tough, and the results conform to the results in reviewed literature.

4.2 AHM-2 (CoFeNi, 1 wt.% WC)

The second ternary alloy-based composite synthesized is designated as AHM-2 which comprises of CoFeNi as matrix and WC as reinforcement. The loading fraction of reinforcement was 1 wt.%.

4.2.1 Microstructure Characterization

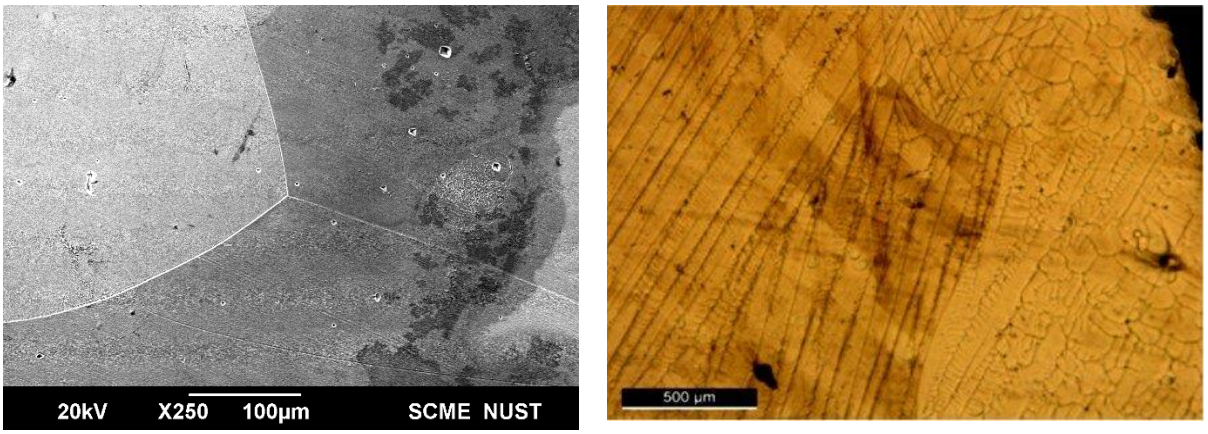

Figure 4. 4: (Left) SEM Micrograph of AHM-2 (as-cast CoFeNi + 1wt.% WC); (Right) Optical Micrograph of AHM-2 (as-cast CoFeNi + 1wt.% WC)

Table 4. 5: Elemental composition of AHM-2 (at. 1 % WC) from EDS

EDS Analysis of CoFeNi-1 wt.% WC		
Element	Weight %	Atomic %
C K	4.4	18.3
Fe K	31.0	27.6
Co K	32.4	27.4
Ni K	31.0	26.3
W L	1.2	0.3

SEM and OM images show the presence of a single phase throughout the matrix. The dark region in the OM image is not another phase but a result of improper etching. With the addition of WC, no other phase was formed in the composite as seen in the micrographs. Grains began to evolve due to the addition of WC in

CoFeNi. Elongated grains are visible in the OM images. EDS analysis confirms the presence of equimolar composition of CoFeNi matrix and the presence of added wt.% of WC.

4.2.2 Crystal Structure Characterization

The peaks (111), (200) and (220) are typical FCC peaks in the XRD plot which confirms the complete formation FCC phase in the composite. Peaks of WC are not visible because its intensity was very low due to the small added amount, therefore it got removed during the noise cancellation of data. The reference graph in figure 4-7 shows that peaks of WC should be present between 32-36 degrees. To resolve the problem of WC peak, a selective slow scan was performed from 30-45 degrees for 90 minutes to get a better resolution of the peaks in the area but still, due to the low amount of WC, its peak was not obtained. The indexing of peaks confirmed that WC was present in the sample, but its peak was not visible in the graph. [7]

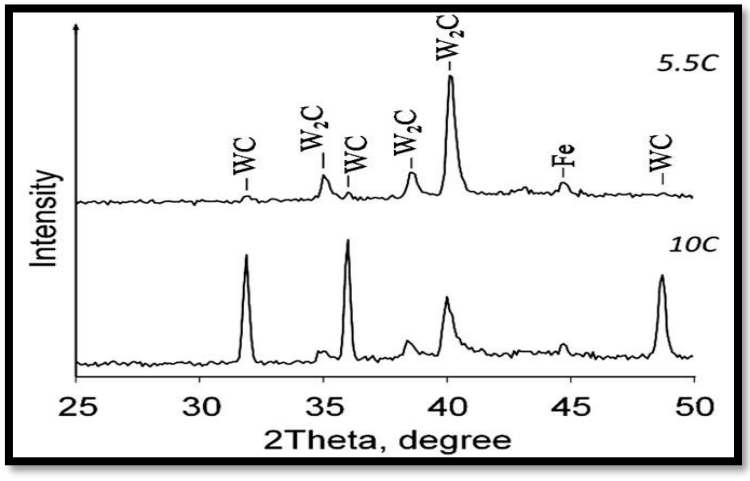

Figure 4. 5:Reference XRD plot of WC [7]

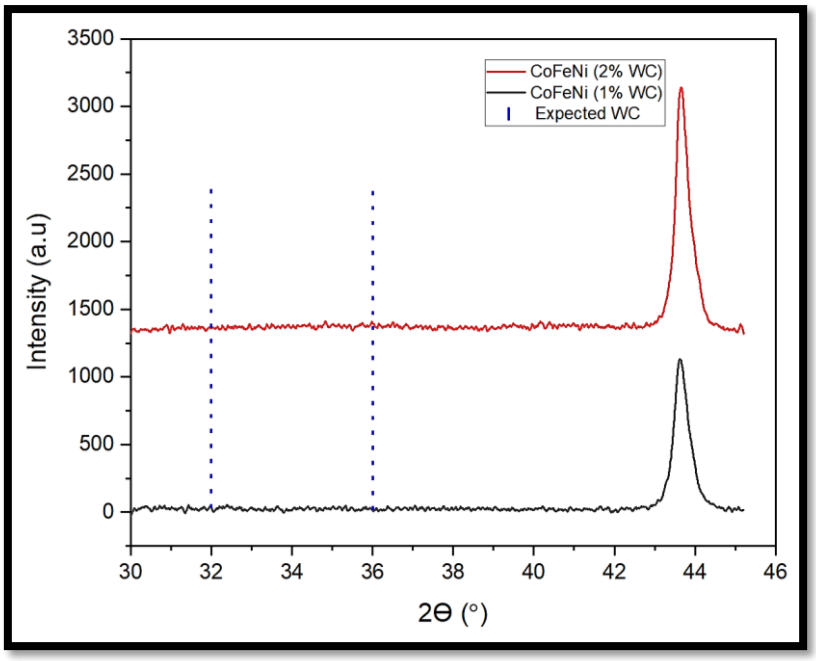

Figure 4. 6: Selective angle slow scan (300-450)

4.2.3 Mechanical Characterization

The testing parameters of Micro-Vickers Hardness (HV) were like AHM-1 i.e., 5 N load and 10 seconds dwell time. The obtained average value was 138 ± 5 HV showing that the hardness of the CoFeNi matrix had increased due to the addition of 1wt.% of WC.

The load and dwell time in Macro-Vickers Hardness (HV) was 300 N and 10 seconds respectively. A value of 134.9 ± 5 HV was obtained from the test which also confirmed the increase in hardness of the composite like Micro-Vickers hardness test.

The difference in these values is because the size of indent is different, indent of Macro-Vickers is larger than that of Micro-Vickers therefore it covers a larger area of the sample and the probability of the presence of WC particles is high which will give the hardness value closer to the true value.

Compression test was performed under similar conditions and test parameters of AHM-1. 01 specimen was tested to find the yield strength of the composite. A yield strength of 137.4 ± 4 N/mm^2 was obtained from this sample. The sample did not fracture till 83% of the strain and the test was stopped at this point.

4.3 AHM-3 (CoFeNi, 2 wt.% WC)

The third ternary alloy-based composite synthesized is designated as AHM-3 which comprises of CoFeNi as matrix and WC as reinforcement. The loading fraction of reinforcement was 2 wt.%.

4.3.1 Microstructure Characterization

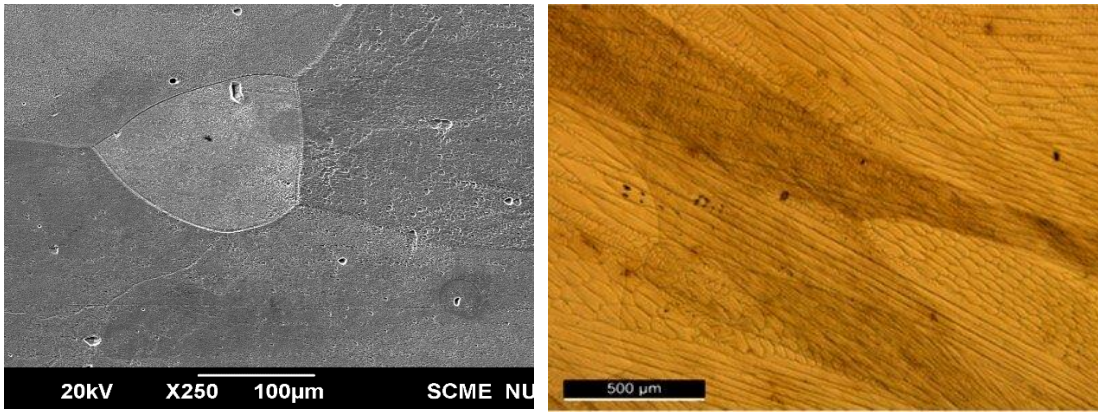

Figure 4. 7: (Left) SEM Micrograph of AHM-3 (as-cast CoFeNi + 2wt.% WC); (Right) Optical Micrograph of AHM-3 (as-cast CoFeNi + 2wt.% WC)

Table 4. 6: Elemental composition of AHM-3 (at. 2 % WC) from EDS

EDS Analysis of CoFeNi-2 wt.% WC		
Element	**Weight %**	**Atomic %**
C K	4.6	18.9
Fe K	31.1	27.7
Co K	32.4	27.3
Ni K	30.2	25.6
W L	1.8	0.5

The images from SEM and OM show the presence of a single phase in the microstructure. OM images show elongated grains that conform to the microstructure in the literature. SEM show a greater number of grain boundaries in the microstructure which is an evidence of grain size refinement with the increasing amount of WC reinforcement in the matrix. EDS analysis confirms the

presence of equimolar composition Cobalt, Iron and Nickel and approximately 2wt.% of WC.

4.3.2 Crystal Structure Characterization

XRD test parameters were like the other 2 samples i.e., scan angle from 20-80 degrees for 90 minutes. Peaks obtained from the test conformed to the peaks of a typical FCC structure which confirmed its formation in AHM-3. Due to low intensity of WC peak, it got removed during background noise cancellation of he obtained data. But the presence of WC in the microstructure was confirmed during the indexing of the XRD peaks. To better resolve the peaks, a selective slow scan was also performed on AHM-3 from 30-45 degrees angle for 90 minutes but still, WC peak is not visible in the XRD plot of selective scan.

4.3.3 Mechanical Characterization

Micro Vickers (HV) and Macro Vickers (HV) hardness test was performed on the AHM-3 like AHM-1 and AHM-2. Upon 2 wt.% addition of WC, the Micro Vickers and Macro Vickers hardness was found to be 147.3 ± 6 HV and 151.5 ± 5 HV respectively. The value of hardness has increased with the increase in loading fraction of reinforcement.

Yield strength value 167.3 ± 6 N/mm^2 was obtained from compression test performed. This also indicates the increase in strength with the addition of increasing amount of WC.

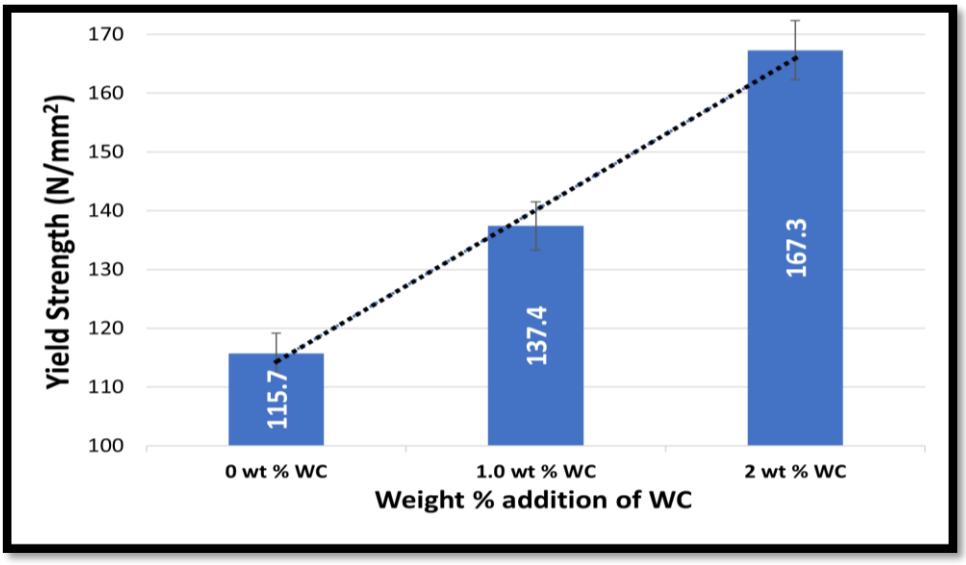

Figure 4. 8: Comparison of yield strengths (N/mm2) at I x 10-3 m/sec strain rate of the synthesized systems

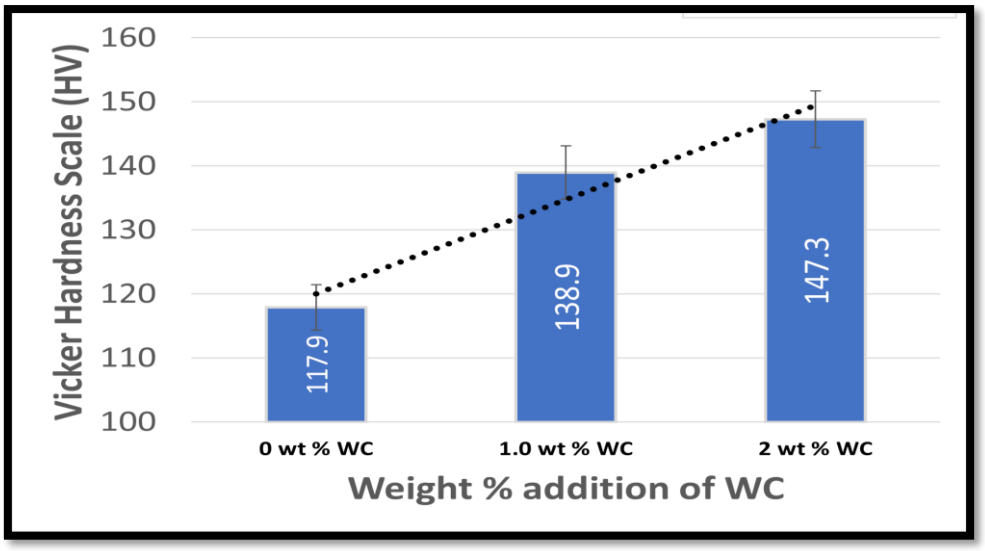

Figure 4. 9: Micro-hardness trend with varying load fraction of WC in CoFeNi matrix at 0.5kgf load and 10 sec dwell time

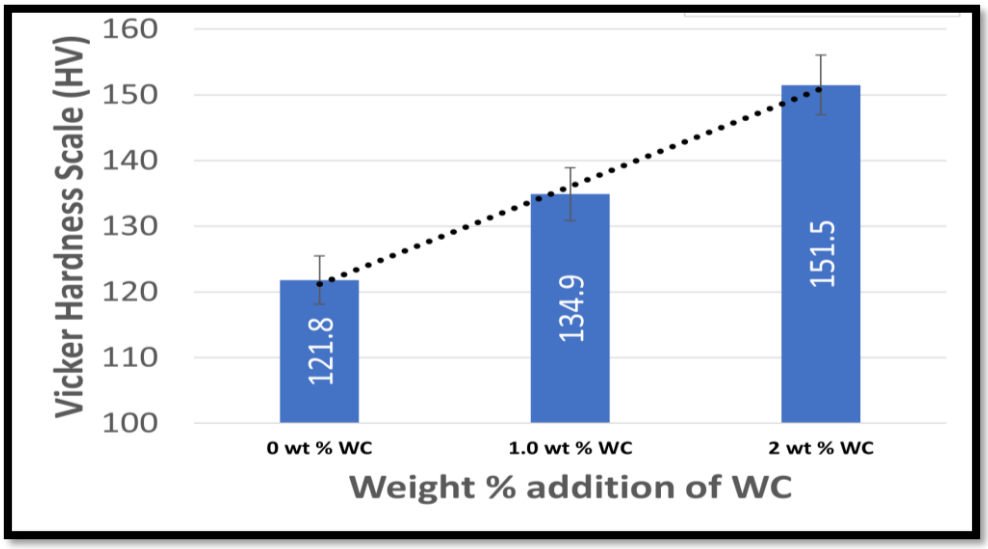

Figure 4. 10: Macro-hardness trend with varying load fraction of WC in CoFeNi matrix at 30 kgf load and 10 sec dwell time

4.4 Conclusion of the chapter

Ternary alloy-based composites were developed through the inclusion of different weight percent of WC. The microstructure, crystal structure and mechanical characterization of all the synthesized systems were carried out. The strength and ductility combination of the composite increased as with 2 weight percent addition of WC, yield strength of the ternary alloy matrix increased from 115.7 N/mm^2 to 167.3 N/mm^2 without significant decrease in ductility. The percentage strain observed in CoFeNi + 2 wt.% WC was 83% where the test was stopped due to limitation of the machine.

CONCLUSION

Several Alloy based composites were developed using vacuum arc melting process and their evaluation was done based on microstructure, crystal structure, compositional and mechanical characterization. Various reinforcements were used to see their effect on composite properties. In this project, effect on strength and ductility combination was studied with the addition of different weight percent of WC. A good strength and ductility combination is required in every application which is difficult to achieve. As the strength of material is increased, its ductility is compromised simultaneously.

The composites synthesized showed increased strength with the addition of WC and a lesser decrease in ductility is observed. The microstructures of the composite exhibited grain refinement with subsequent increase of WC reinforcement. This refinement of grains led to the increase in the strength of the material but due to lesser addition of amounts no significant variation was observed.

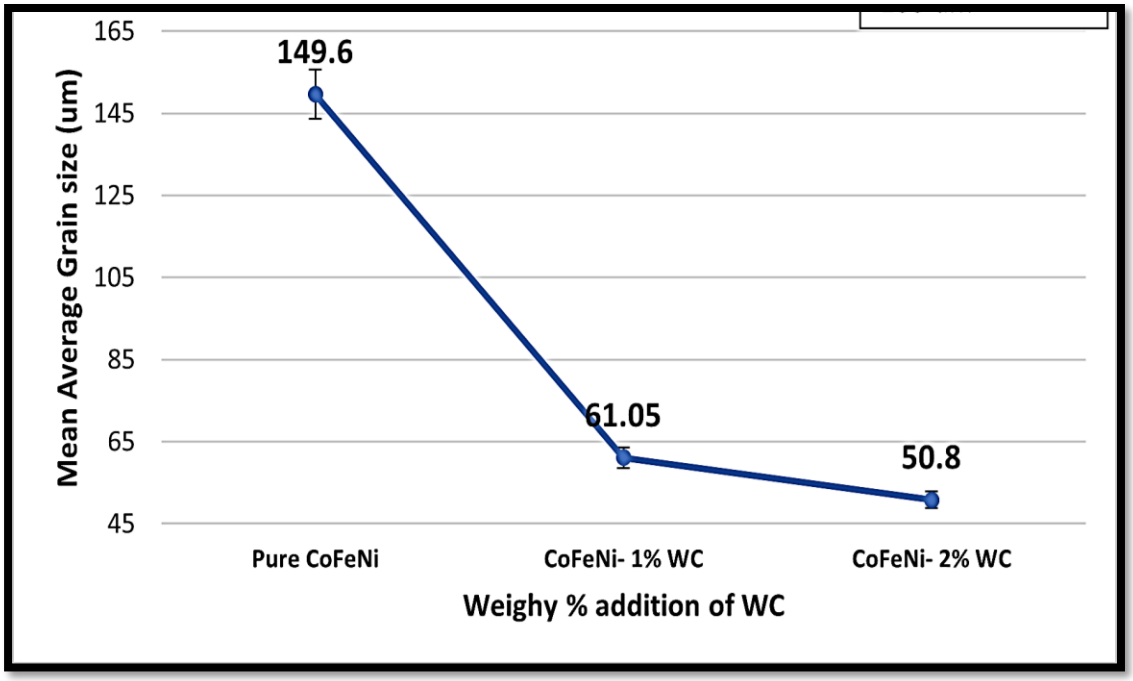

Figure 5-1: Comparison of grain size of all systems at 100 um magnification during the research

5.1 Impediments during synthesis and sample preparation

- WC was difficult to incorporate in the alloy during melting due to splashing issues
- Polishing of the sample was not possible with alumina suspension, diamond paste had to be ordered and used instead.

REFERENCES

[1] Rashad, M.., Pan, F., Yu, Z., Asif, M., Lin, H., & Pan, R. (2015). Investigation on microstructural, mechanical and electrochemical properties of aluminum composites Progress in natural science: materials reinforced with graphene nanoplatelets. international, 25(5), 460-470.

[2] Home. (n.d.), (2019, October 6) Online text https://www. globenewswire.com/news-release/2020/06/03/2042677/0/en/AerospaceComposites-Market-Size-Worth-USD-29-69-Billion-by-2026-COVID1 9-ImpactAnalysis-Global-Industry-Share-Growth-Rate-Fortune-Business-Insights.html

[3] Shah, K. B., Kumar, S., & Dwivedi, D. K. (2007). Aging temperature and abrasive wear behaviour of cast Al-(4%, 12%, 20%) Si—0.3% Mg alloys. Materials & design, 28(6), 1968-1974.

[4] Wang, J., Li, Z., Fan, G., Pan, H., Chen, Z., & Zhang, D. (2012). Reinforcement with graphene nanosheets in aluminum matrix composites. Scripta Materialia, 66(8), available at $94-597.

[5] Kala, H., Mer, K. K. S., & Kumar, S. (2014). A review on mechanical and tribological behaviors of stir cast aluminum matrix composites. Procedia Materials Science, 6, 1951-1960.

[6] Bastwros, M., Kim, G. Y., Zhu, C., Zhang, K., Wang, S., Tang, X., & Wang, X (2014). Effect of ball milling on graphene reinforced Al6061 composite fabricated by semi-solid sintering. Composites Part B: Engineering, 60, 111-118

[7] Surappa, M. K. (2003). Aluminium matrix composites: Challenges and opportunities. Sadhana, 28(1-2), 319-334. [8] Darolia, R. (1991). NiAl alloys for high-temperature structural applications JoM, 43(3), 44-49.

[8] Cheng, S., Spencer, J. A., & Milligan, W. W. (2003). Strength and tension/compression asymmetry in nanostructured and ultrafine-grain metals. Acta Materialia, 51(15), 4505-4518.

[9] Cheng, S., Ma, E., Wang, Y. M., Kecskes, L. J., Youssef, K. M., Koch, C. C., .. & Han, K. (2005). Tensile properties of in situ consolidated nanocrystalline Cu. Acta materialia, 53(5), 1521-1533.

[10] X. Xiang, G. Wang, X. Zhang, Y. Xiang and H. Wang, "Individualized Pixel Synthesis and Characterization of Combinatorial Materials Chips", *Engineering*, vol. 1, no. 2, pp. 225-233, 2015. Available: 10.15302/j-eng-2015041.

[11] Li, A. Wang and C. Liu, "Composition dependence of structure, physical and mechanical properties of FeCoNi(MnAl) x high entropy alloys", *Intermetallics*, vol. 87, pp. 21-26, 2017. Available: 10.1016/j.intermet.2017.04.007

[12] Wu, X., Yuan, F., Yang, M., Jiang, P., Zhang, C., Chen, L.. ... & Ma, E. (2015 Nanodomained nickel unite nanocrystal strength with coarse-grain ductility, Scientf. reports, 5, 11728.

[13] Deng, Y., Tasan, C. C., Pradeep, K. G., Springer, H., Kostka, A., & Raabe, f) (2015). Design of a twinning-induced plasticity high entropy alloy. Acta Materialia, 94 24-133, '

[14] Rajasekhara, S., Karjalainen, L. P., Kyréldinen, A., & Ferreira, P. J. (2011) Development of stainless steels with superior mechanical properties: a correlation between structure and properties in nanoscale/sub-micron grained austenitic stainless Steel. In Advanced Steels (pp. 371-384). Springer, Berlin, Heidelberg.

[15] Ye, Y. F., Wang, Q., Lu, J., Liu, C. T., & Yang, Y. (2016). High-entropy alloy. challenges and prospects. Materials Today, 19(6), 349-362.

[16] Cantor, B., Chang, I. T. H., Knight, P., & Vincent, A. J. B. (2004), Microstructural development in equiatomic multicomponent alloys. Materials Science and Engineering: A, 375, 213-218.

[17] Yeh, J. W., Lin, S. J., Chin, T. S., Gan, J. Y., Chen, S. K., Shun, T. T., ... & Chou, S. Y. (2004). Formation of simple crystal structures in Cu-Co-Ni-Cr-Al-Fe-Ti-V alloys with multiprincipal metallic elements. Metallurgical and Materials Transactions A, 35(8), 2533-2536.

[18] Yeh, J. W., Chen, S. K., Lin, S. J., Gan, J. Y., Chin, T. S., Shun, T. T., ... & Chang, S. Y. (2004). Nanostructured high-entropy alloys with multiple principal elements: novel alloy design concepts and outcomes. Advanced Pngineering Materiale, 6(5), 299-303.

[19] Tomilin, I. A., & Kaloshkin, S. D. (2015). 'High entropy alloys' 'sems impossible' regular solid solutions, Materials Science and Technology, 31(10), 1231 1234, Scientific Group Thermodata Europe (SGTE). (1999). Thermodynamic properties of inorganic materials. Landolt-Boernstein New Series, Group IV.

[20] Chuang, M. H., Tsai, M. H., Wang, W. R., Lin, 8. J., & Yeh, J. W. (2051). Microstructure and wear behavior of AlxCol. 5CrFeNil. 5Tiy high-entropy alloys. Acta Materialia, 59(16), 6308-6317.

[21] Yeh, J.W ., Chang , S.Y. , Hong , Y.D. , Chen , S. K, & Lin , S.J. (2007) Anomalous decrease in X-ray diffraction intensities of Cu-Ni-Al-Co-Cr—Fe-Si alloy systems with multi-principal elements. Materials chemistry and physics, 103(1), 41-46.

[22] Tsai, K.-Y., Tsai, M.-H., & Yeh, J.-W. (2013). Sluggish diffusion in Co—Cr—Fe Mn-Ni high-entropy alloys. Acta Materialia, 61(13), 4887-4897. Zhang, Y., Zuo, T. T., Tang, Z., Gao, M. C., Dahmen, K. A., Liaw, P. K.. & La,

[23] Yeh, J. W., Chang, S. Y., Hong, Y. D., Chen, S. K., & Lin, S. J. (2007). Anomalous decrease in X-ray diffraction intensities of Cu-Nt-AlCo-Cr-Fe-Si alloy systems with multi-principal elements. Materials chemistry and physics, 103(1), 41-46.

[24] Huan , P.K . , Yeh , J.W. , & Wong , M.S. (2004) element alloys with improved oxidation and wear resistance for thermal spray coating. Advanced Engineering Materials, 6(1-2), 74-78.

[25] Du, Y., Lu, Y., Wang, T., Li, T., & Zhang, G. (2012). Effect of electromagnetic Stirring on microstructure and properties of Al0. 5CoCrCuFeNi alloy. Procedia Engineering, 27, 1129-1134. [41] Wang, Y. P., Li, B. S., & Fu, H. Z. (2009). Solid Solution or Intermeitallics in a High-Entropy Alloy. Advanced engineering materials, 11(8), 641-644.

[26] Zhou, Y. J., Zhang, Y., Wang, Y. L., & Chen, G. L. (2007). Solid solution alloys of Al Co Cr Fe Ni Ti x with excellent room-temperature mechanical properties. Applied physics jetters, 90(18), 181904.

[27] Zhang, Y., Zuo, T., Cheng, Y., & Liaw, P. K. (2013). High-entropy alloys with high saturation magnetization, electrical resistivity, and malleability. Scientific reports, 3, 1455,

[28] Tsai, M. H., & Yeh, J. W. (2014). High-entropy alloys: a critical review. Materials Research Letters, 2(3), 107-123.

[29] Callister, W. D., & Rethwisch, D. G. (2007). Materials science and engineering: an introduction (Vol. 7, pp. 665-715). New York: John wiley & sons.

[30] Zhu. J.M., Fu, H. M., Zhang, H. F., Wang, A. M., Li, H., & Hu, Z. Q. (2010). Microstructures and compressive properties of multicomponent AlCoCrFeNiMox alloys. Materials Science and Engineering: A, 527(26), 6975-6979.

[31] Zhu. J. M.. Fu, H. M., Zhang, H. F., Wang, A. M., Li, H., & Hu, Z. Q. (2010). Synthesis and properties of multiprincipal component AlCoCrFeNiSix alloys. Materials Science and Engineering: A, 527(27-28), 7210-7214.

[32] Zhu, J. M., Fu, H. M., Zhang, H. F., Wang, A. M., Li, H., & Hu, Z. Q. (2011). Microstructure and compressive properties of multiprincipal component AlCoCrFeNiCx alloys. Journal of Alloys and Compounds, 509(8), 3476-3480.

[33] Chou, H.-P.; Chang, Y.-S.; Chen, S.-K.; Yeh, J.-W. Microstructure, thermophysical and electrical properties in AlxCoCrFeNi (0 < x < 2) high-entropy alloys. Mater. Sci. Eng. B 2009, 163, 184-189

[34] Zhu, J.M.; Fu, H.M.; Zhang, H.F.; Wang, A.M.; Li, H.; Hu, Z.Q. Synthesis and Properties of multiprincipal component AlCoCrFeNiSix alloys. Mater. Sci. Eng. A 2010 ,527, 7210-7214,

[35] Valency effects and relative solubilities in transition metal alloys D. A. Good, and L. 4. Bennett National Bureau of Standards, Washington DC, 20234 R. E, Wat an Brookhaven National Laboratory. "

[36] Kyeong Ho Kong et.al. Microstructural Features of Multicomponen FeCoCrniSix Alloys. Regular article: Applied Microscopy, Korean society of microscopy. pISSN 2287-5123:eISSN 2287-4445. _http://dx.doi.org/10.9729, AM.2015.45.1.32

[37] Aijun Zhang et al. Microstructure, mechanical properties and _tribologica) performance of CoCrFeNi high entropy alloy matrix self-lubricating composite. Materials and Design 114 (2017) 253-263.

[38] Z. Wu, H. Bei, G.M. Pharr, E.P. George, Temperature dependence of the mechanical properties of equiatomic solid solution alloys with face-centered cubic crystal structures, Acta Mater 81 (2014) 428-441.

[39] Liang Weia et al. Effect of roughness on general common and puting af [PeCoCrNijO.89WC)O. UT high-entropy alloy composite i 35 wis Nac soliton, Corrosion Science 146 (2019) 44-57,

[40] Christodoulou ef al. Arc-melting process for forming metalle-sceund phat composites, US Patent Number 5,093,148 dated Mar. 3, 1992

[41] The balance, Metallographic Etching, (2019, October 6) Online text avatlable af https://Awww.thebalance.com/metallographte-etching-2340003

[42] J. Jerosch and R. Reichelt, “Scanning electron microscopy studies of momhaloge changes in chemically stabilized ultrahigh molecular weight pohethy lene,” Biomedizinische Technik. Biomedical engineering, vol. 42. pp. 358 362, 1997,

[43] C. W. Oatley, W. c. Nixon, and R. F. W. Pease, “Scanning Electron Microscopy.” Advance Electronics Electron Physics, vol. 21, pp. 181-247, 1965,

[44] R. Schmitt, “Scanning Electron Microscope,” in CIRP Encyclopedia of Production Engineering, L. Laperriére and G. Reinhart, Eds. Berlin, Herdclberg: Spnnger Berlin Heidelberg, 2014, pp. 1085-1089.

[45] H. Stanjek and W. Hausler, “Introduction To Powder/ Poly crystalline Diffraction,” Hyperfine Interactions, vol. 154, pp. 107-119, 2004.

[46] X-ray Powder Diffraction (XRD), (2019, October 6). Online text available at https://serc.carleton.edu/research_education/geochemsheets/techniques/XRD html

[47] Home. (n.d.), (2019, October 6) Online tert available at https://www. labtesting.com/services/materials-testing/metallurgical-testing/mienohandne Ss-testing/